Startup, Transition Core, and Molybdenum-99 Production Upgrade Analyses for Low-Enriched Uranium Fuel Conversion at the University of Missouri Research Reactor

---

A Dissertation

presented to the Faculty of the Graduate School

at the University of Missouri-Columbia

In Partial Fulfillment

of the Requirements for the

Degree Doctor of Philosophy

---

by

WILSON COWHERD

Dr. John Gahl, Dissertation Supervisor

JULY 2020

The undersigned, appointed by the Dean of the Graduate School, have examined the dissertation entitled

STARTUP, TRANSITION CORE, AND MOLYBDENUM-99 EXPERIMENT UPGRADE ANALYSES FOR LOW ENRICHED URANIUM FUEL CONVERSION AT THE UNVERSITY OF MISSOURI RESEARCH REACTOR

presented by Wilson Cowherd,

a candidate for the degree of doctor of philosophy,

and hereby certify that, in their opinion, it is worthy of acceptance.

_____

Professor John Gahl

_____

Professor J. David Robertson

_____

Professor William Miller

_____

Professor Nickie Peters

_____

Dr. John Stillman

ACKNOWLEDGEMENTS

I would like to thank the MURR and Argonne teams that supported me every step of the way during this research. In particular, I would like to thank Les Foyto, Dr. Nickie Peters, Dr. Das Kutikkad, Charlie McKibben, and Dr. John Gahl from MURR, and Dr. John Stillman and Dr. Erik Wilson from Argonne National Laboratory. This research would not have been possible without them.

This research is sponsored at the University of Missouri by the U.S. Department of Energy, National Nuclear Security Administration Office of Material Management and Minimization Reactor Conversion Program under contract 7J-30010 with Argonne National Laboratory.

Table of Contents

List of Figures

List of Tables

STARTUP, TRANSITION CORE, AND MOLYBDENUM-99 EXPERIMENT UPGRADE ANALYSES FOR LOW ENRICHED URANIUM FUEL CONVERSION AT THE UNVERSITY OF MISSOURI RESEARCH REACTOR

Wilson Cowherd

Dr. John Gahl, Dissertation Supervisor

ABSTRACT

Under the direction of the United States Department of Energy (DOE) National Nuclear Security Administration (NNSA) Office of Material Management and Minimization (M3) Reactor Conversion Program, the University of Missouri Research Reactor (MURR®) plans to convert from highly enriched uranium (HEU) fuel to low-enriched uranium (LEU) fuel. Low-power physics startup test predictions, transition core planning, and analysis for a proposed fission-based molybdenum-99 production upgrade were done in support of LEU fuel conversion.

As a first step to LEU fuel conversion, low-power physics tests will be performed to calculate reactor physics parameters. These parameters include flux distributions, coefficients of reactivity, and critical assembly measurements. To facilitate this test, reactor physics calculations were performed using MCNP5 to predict the values of these parameters. Implications of these predictions and areas of uncertainty in the prediction analysis are also discussed.

Once MURR completes the testing of the initial LEU core, MURR will enter into a series of transition cycles until steady-state mixed-burnup operation is reached. A Python program was developed that incorporated the constraints of MURR operation while minimizing the time MURR will have to operate atypically during the transition cycles. The impacts of the transition cycles on experiment performance are reported, as well as the number of fuel elements needed.

Finally, preliminary analysis on a proposed molybdenum-99 production device at MURR was performed. This analysis shows the impact on the reactor power distribution with implications to predicted safety margins as a part of the larger scope of the experiment analysis.

I. INTRODUCTION

A. BACKGROUND

The international non-proliferation community aims to minimize the amount of highly enriched uranium (HEU) that could be diverted and used for nuclear weapons. In this context most research and test reactors, both domestic and international, have started a program of conversion to the use of low-enriched uranium (LEU) fuel. For decades, the National Nuclear Security Administration (NNSA) Office of Material Management and Minimization (M3) Reactor Conversion Program (formerly, the Global Threat Reduction Initiative (GTRI) and the Reduced Enrichment for Research and Test Reactors (RERTR) programs) has sponsored efforts to develop and qualify fuel, design and fabricate fuel elements, model fuel cycles and reactor operations, perform reactor safety analyses, maintain experimental performance and irradiation services, and support regulatory submissions to meet the challenges of reactor conversion [1]. To date, more than 70 reactors worldwide, including 20 in the U. S., have completed conversion to LEU in cooperation with the M3 conversion program [2] [3].

The University of Missouri Research Reactor (MURR®) located in Columbia, Missouri is among six U.S. domestic high-performance research reactors (USHPRR), including one critical facility, that are actively collaborating with the M3 conversion program to convert from the use of HEU to LEU fuel. MURR started collaborating with the USHPRR conversion project in 2006 and must address unique challenges in converting to LEU fuel. MURR first began operations in 1966, and for more than 40 years, MURR has provided predicable and stable irradiation services during a weekly operating cycle of 6.3 full-power days. Consequently, demonstrating adequate safety margins and maintaining existing experimental performance are key to the regulatory and

operational decisions to convert to LEU. Much of the insight from the program informs the decisions made by MURR in its fuel conversion effort.

A new type of LEU fuel based on an alloy of uranium and molybdenum (U-10Mo) is expected to allow the conversion of those USHPRRs requiring high density fuel. The USHPRR Conversion project is completing irradiation and post-irradiation testing of the very high density U-10Mo fuel under a planned and documented fuel qualification effort with the U.S. Nuclear Regulatory Commission for use in three of the USHPRR, including MURR [4]. For one other USHPRR additional high-power testing of the U-10Mo fuel is needed. For the sixth USHPRR, qualification of existing uranium-silicide fuel at relevant power densities is needed [5]. Working in collaboration with M3, MURR has completed preliminary fuel element design, experimental performance calculations, and safety analyses for both steady-state and transient/accident conditions following conversion to this LEU fuel for transition to equilibrium fuel cycle operations with mixed-burnup cores that are typical for MURR [6] [7] [8].

As a part of this collaboration, significant progress has been made in the effort to convert MURR to LEU fuel. Conceptual design analysis based on U-10Mo monolithic LEU fuel was completed in 2012 [8]. The proposed LEU element design was optimized based on feedback from the fuel fabricator. Studies with the preliminary LEU fuel element design have concluded that for an equilibrium LEU core, in conjunction with an increase in power level from 10 to 12 MW_{th}, MURR will maintain an acceptable level and spectrum of key neutron fluxes and reaction rates to meet the scientific mission of the facility. The preliminary LEU design will also allow for current operating fuel cycle lengths to be maintained for effective use of the facility and preserve safety margins during steady-state operations and transient conditions. The MURR and Argonne National Laboratory (ANL) teams are continuing to work toward realization of this

conversion along with other national laboratories and organizations working on fuel fabrication and fuel irradiation testing [4] [9] [10] [11].

MURR is a light-water moderated and cooled, pressurized, reflected, open-pool type reactor. MURR's current maximum licensed power level is 10 MW with a peak unperturbed neutron flux in the center flux trap of 6.0×10^{14} n/cm^2-s. The reactor is controlled using four BORAL® control blades and one stainless steel regulating blade, with beryllium and graphite reflectors to improve performance. The forced primary coolant flow rate is 237 liters per second at 586 kPa with a temperature 49 °C at the inlet and 59 °C at the outlet. The forced pool coolant flow rate is 76 liters per second, with a temperature of 38 °C inlet and 41 °C outlet [7]. The MURR reactor core assembly is shown in Figure 1.

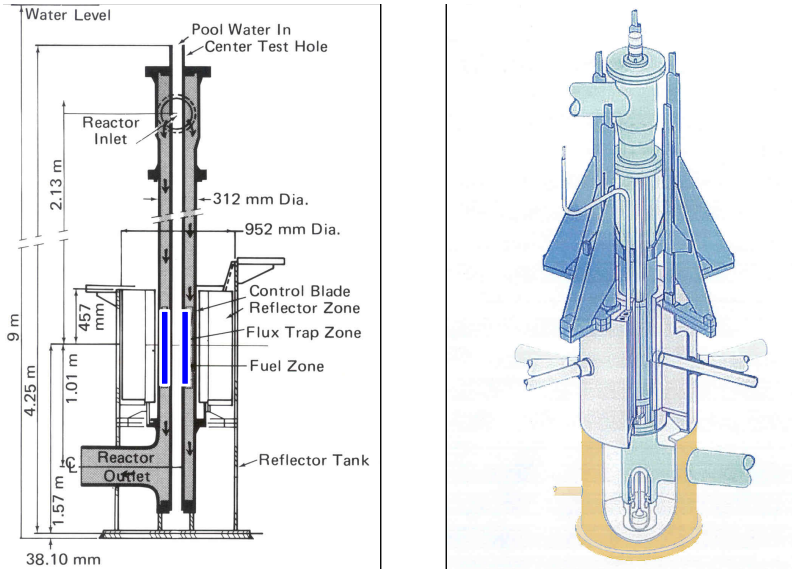

Figure 1: MURR Reactor Core Assembly

The MURR core has a fixed geometry consisting of eight fuel elements, each having identical physical dimensions. The fuel elements are placed vertically around an annulus

between two cylindrical aluminum reactor pressure vessels. A cross-sectional view of the MURR reactor core is shown in Figure 2.

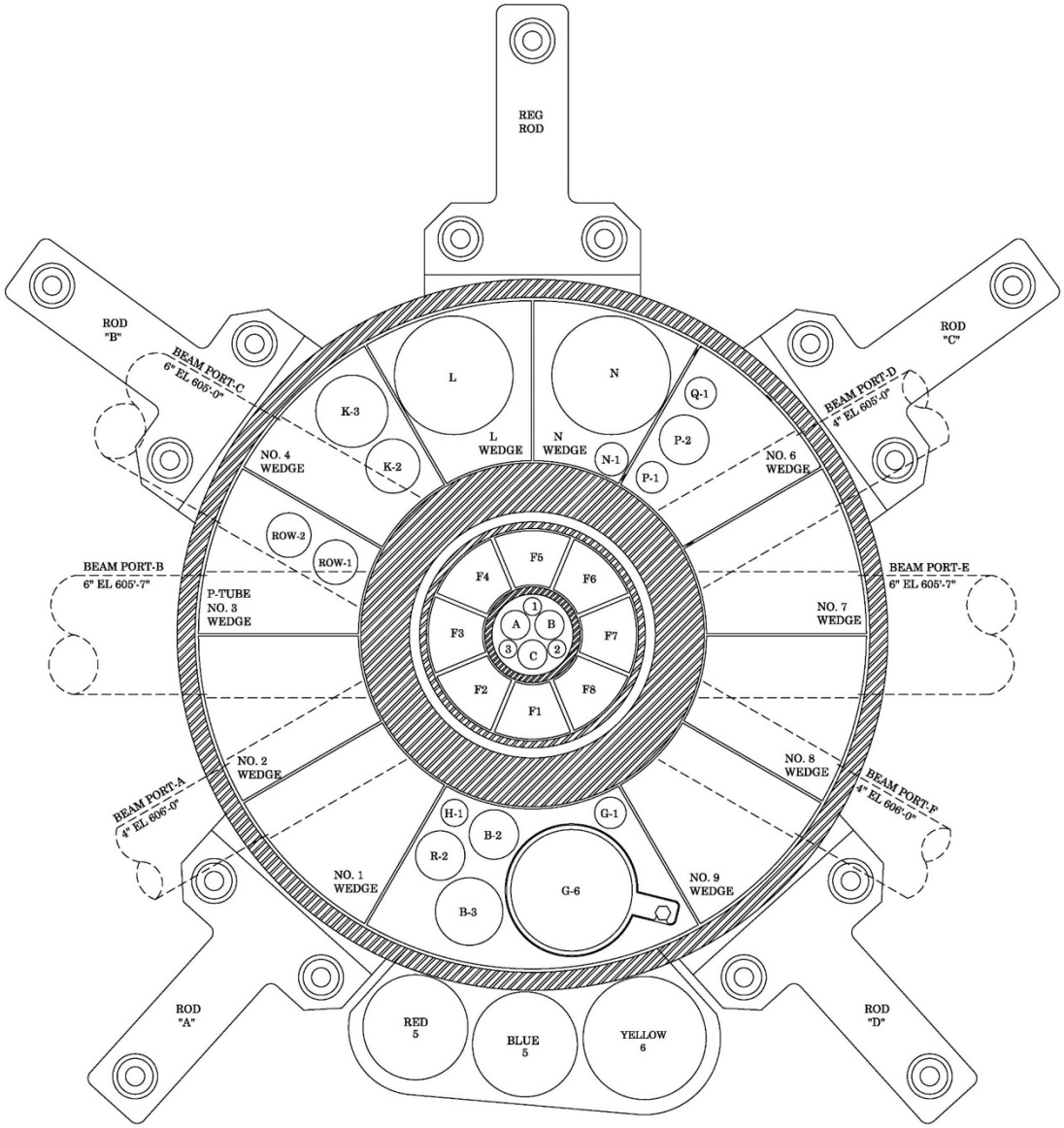

Figure 2: Cross-Sectional View of MURR Reactor Core

The current HEU fuel element used in MURR has 24 curved plates that form a 45-degree arc. The HEU fuel plates are 0.127 cm thick. The fuel meat is 0.0508 cm thick in each plate and

consists of uranium-aluminide (UAl_x) dispersion fuel containing uranium with a ^{235}U enrichment of approximately 93%. The HEU plates are nominally clad with 0.0381 cm of AA6061. The fuel plates are 64.77 cm long, with an active fuel meat length of 60.96 cm. While the plate and meat width vary by plate, each plate has two unfueled edges that are 0.3683 wide [7].

Figure 3 andFigure 4 provide illustrations of the MURR preliminary LEU fuel element design. As for the HEU element, the fuel plates are swaged into two AA6061 side plates that are 0.381 cm thick, 8.0264 cm wide, and 80.645 cm long. The plates fit into grooves cut into the side plate that are 0.1905 cm deep. A comb is attached over the fuel plates at their top and bottom to provide additional structural support and help maintain fuel plate spacing. The side plates are attached to the top and bottom end fittings. Rollers on the inside and outside edges of the end fittings facilitate insertion of the elements into the annular pressure vessel of the MURR. The rollers also ensure that the minimum outer channel clearances are maintained. The overall length of the element is 82.55 cm.

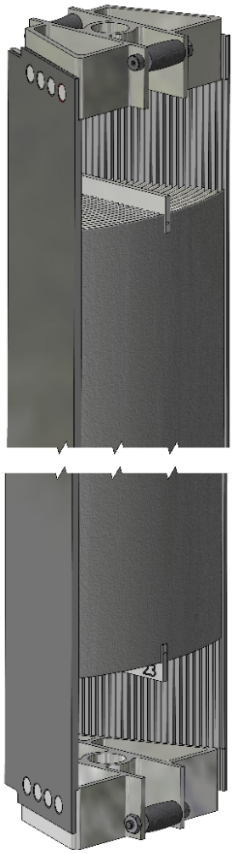

Figure 3: Overview of MURR Fuel Element

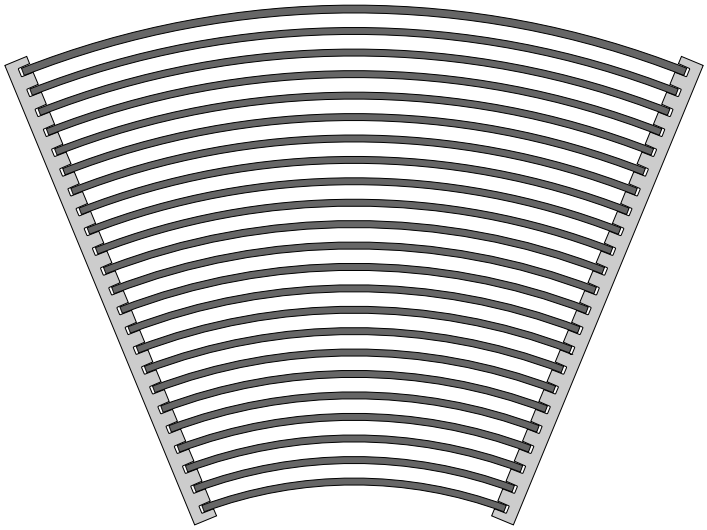

Figure 4: Cross-Sectional View of MURR Fuel Element

In order to meet the reactivity requirements of the MURR operating cycle with LEU fuel, it is necessary to have a much higher uranium density than the currently qualified UAl_x or silicide dispersion fuels. U-10Mo monolithic fuel that can provide a uranium density of 15.3 gU/cm^3 has been selected for the LEU fuel, pending successful fuel qualification. A fuel element design with U-10Mo LEU fuel, along with a 20% power uprate following conversion, was found to safely meet the MURR operating cycle requirements and maintain existing reactor performance [7].

The preliminary LEU fuel element has 23 fuel plates. Each fuel plate is 64.77 cm long, with a 60.96 cm fueled length. The unfueled edge on each side of the fuel plates is 0.3683 cm, of which no more than 0.1905 cm extends into a groove cut into the element side plates. The other portions of the element construction (e.g., side plate length, width, and thickness; and end

fittings) will be identical to the HEU fuel element. The LEU fuel core thickness, the zirconium interlayer, and the AA6061 cladding thickness are presented in Table I along with a summary comparison with the HEU fuel in Table II.

Fuel Plate Dimension	**Location**	**Nominal Value [inches (mm)]**
Fuel Core Thickness	Plate 1	0.009 (0.229)
	Plate 2	0.012 (0.305)
	Plate 3	0.016 (0.406)
	Plates 4–22	0.020 (0.508)
	Plate 23	0.017 (0.4318)
Zirconium Interlayer	All Plates	0.001 (0.025)
AA6061 Cladding Thickness	Plate 1	0.0165 (0.419)
	Plate 2	0.015 (0.381)
	Plate 3	0.013 (0.330)
	Plates 4–22	0.011 (0.279)
	Plate 23	0.015 (0.381)
Plate Thickness	Plate 1–22	0.044 (1.118)
	Plate 23	0.049 (1.225)
Coolant Channel Gap (for channels 1 and 24, the dimension is from plate to the roller)	Channel 1	0.0805 (2.045)
	Channels 2–5	0.093 (2.362)
	Channels 6–19	0.092 (2.337)
	Channels 20–23	0.093 (2.362)
	Channel 24	0.0805 (2.045)

Table I: LEU Fuel Element Specifications [7]

Description	**Nominal Value HEU**	**Nominal Value LEU**
Fuel Content (grams ^{235}U per element / grams U per element)	775 / 833	1507 / 7630
Type of Fuel	Aluminide-UAl_x mostly UAl_3 Phase	U-10Mo Monolithic Alloy
Fuel Density (grams of ^{235}U loaded per cubic centimeter)	1.43	3.03
Boron Content (natural boron per element)	Trace Impurities	Trace Impurities
Peak Local Burnup Density at Discharge (fissions per cubic centimeter)	$< 2.3 \times 10^{21}$	$< 3.4 \times 10^{21}$
Element Burnup at Discharge (MWd per element)	≈ 150	180

Table II: LEU Fuel Comparison with HEU [7]

B. NEUTRONICS METHODS

For the startup analysis, transition cycles analysis, and molybdenum-99 production upgrade analysis, two main neutron physics codes were used. The first was the Monte Carlo N-Particle (MCNP) radiation transport code [12]. MCNP5 is a general-purpose radiation transport code that can simulate transport of a variety of particles, including neutrons, protons, electrons, and combinations of these particles. MCNP5 has found a wide variety of uses in industry and academia, and is well-validated for reactor use, including regular use at MURR [13]. MCNP5 is able to model three-dimensional geometry in detail, making it ideal for modeling the complex geometry at MURR. In addition to performing criticality calculations, MCNP5 has the ability to "tally" particles in particular cells for a variety of reactions. For example, MCNP5 is able to calculate fission heating and particle flux by tallying the number of particles that interact with a

cell or surface and results in the particular reaction of interest. MCNP's ubiquitous use in the nuclear industry, long history of reliability, and its usability all contributed to the decision to use it for detailed eigenvalue and neutron tally calculations in these analyses.

The second neutronics code that was used for the fuel cycle simulation of the transition core analysis was REBUS-PC [14]. As one solution option, REBUS-PC uses the DIF3D multi-dimensional, multi-group neutron diffusion code to quickly simulate the neutronic environment for each state point of the transition cycle. Diffusion codes generally execute much faster than Monte Carlo neutronics codes, which is preferred for calculating the fuel burnup over the many state points needed for simulating multiple fuel cycles. Furthermore, the θ-R-z geometry option in DIF3D utilizing broad-group cross sections for the fuel, fission products, and structural components prepared with WIMS-ANL [15] was found to be well-suited for modeling the MURR fuel cycle with either HEU or LEU fuel [16] and to provide good agreement for predictions of the core reactivity compared to higher-fidelity MCNP5 models [8]. A database of depleted HEU fuel element compositions generated by REBUS-DIF3D is routinely used at MURR for predicting beginning-of-cycle (BOC) and hot-startup estimated critical control blade positions [17]. The REBUS code uses the neutron flux solution from DIF3D to calculate the composition of the depleted fuel elements which are loaded into the reactor core, and also accounts for radioactive decay during the time the elements are out of the reactor.

For the fuel cycle simulation, it was necessary to model MURR within the limits of the DIF3D geometry capabilities. Some of the more significant simplifications in the DIF3D model of MURR are: homogenized experiments in the experimental positions, homogenization of the fuel and cladding, and banking of the control blades at a height of 58.42 cm, which is the typical position of the control blades at equilibrium xenon conditions. By using this simplified

model, the fuel element burnup in the transition cycles can be simulated with minimal computational effort. The MURR MCNP5 model, by comparison, has much more detail. This model contains the full detailed mapping of MURR, including explicit modeling of specific experiments, critical blade heights, and explicit fuel element design.

While the DIF3D model is not used for detailed critical power distributions, the model does need to accurately represent the neutronic environment at each state point for the depletion of the elements which is calculated by REBUS. It was found that even with the simplified geometry of the DIF3D model, the predicted k_{eff} is in good agreement with the more detailed MCNP5 model. For example, Table III compares the k_{eff} from the DIF3D model with homogenized experiments with the k_{eff} from the more detailed MCNP5 model for a case with all fresh LEU fuel and the control blades at 58.42 cm withdrawn.

DIF3D	MCNP	Difference
1.07250	1.07294 ± 0.00005	-0.038% Δk/k

Table III: Comparison of DIF3D and MCNP5 Models of MURR with All Fresh LEU Fuel and Control Blades at 58.42 cm Withdrawn

Another point of comparison that is relevant to this analysis is the power distributions predicted by DIF3D and MCNP5. Table IV provides a comparison of the element powers predicted by DIF3D and MCNP5 for a core loaded with eight fresh LEU elements. This comparison was completed as part of the safety analyses of a proposed molybdenum-99 production upgrade in experiment positions in two graphite reflector positions [18]. All other experiment positions were modeled with the same experiments as in the current work. Other than the single change to the experimental configuration of MURR that is located outside the core environment, this analysis is directly applicable to the current transition core analysis and confirms that the DIF3D models reasonably predict the core power distribution relative to the

more detailed MCNP5 models. The results show that all element powers predicted by DIF3D agree within 0.7% of the values predicted by MCNP.

Element Position	DIF3D (MW)	MCNP (MW)	Difference
1	1.465	1.469	-0.3%
2	1.492	1.491	0.1%
3	1.504	1.494	0.7%
4	1.523	1.517	0.4%
5	1.496	1.494	0.1%
6	1.525	1.528	-0.2%
7	1.498	1.508	-0.7%
8	1.497	1.498	-0.1%
Total	12.0	12.0	0.0%

Table IV: Element Power Comparison between DIF3D and MCNP

II. STARTUP TEST PLAN AND PREDICTIONS

A. INTRODUCTION

Non-power reactors licensed by the NRC require a startup test plan as part of any facility modification, including comparisons of measurements with predictions and acceptance criteria, to verify operability prior to resumption of operations [19]. Consequently, a key step in the conversion from HEU to LEU fuel is the startup physics testing of the initial LEU core. These startup tests will ensure that the LEU core performs in a manner consistent with prior analysis and testing for HEU and predictions for LEU. To assist with the startup tests, predictions have also been made to provide insight into key physics parameters and guidance for LEU reactor operations. In this chapter, both the intended startup test plan and predictions for the startup tests are discussed.

Because MURR is regulated by the NRC as a non-power reactor, the guiding document for all licensing decisions, including LEU conversion, is NUREG-1537 [19]. NUREG-1537 "gives guidance to non-power reactor licensees and applicants on the format and content of applications to the Nuclear Regulatory Commission for licensing actions. These licensing actions include…conversions from highly enriched uranium to low-enriched uranium [19]." As a part of the guidance provided in NUREG-1537, a series of low-power startup tests for the initial LEU core is mandated. These tests are meant to ensure that operation with the new fuel is well understood and validate predictions of reactor physics parameters. According to NUREG-1537, the startup plan should include 1) an approach to critical measurement during fuel loading; 2) a plan to determine important operational reactor physics and thermal-hydraulic parameters; and 3)

measurements of magnitudes of area radiation fields. The focus of this chapter is the approach to critical measurement and the experiment plan for reactor physics parameters and the associated predictions.

A startup test plan and predictions were compiled by Julian for MURR for the transition to the current 775g ^{235}U HEU fuel element [20] [21]. These reports provided the analysis of key reactor parameters, a thorough plan for completing startup tests that measure the reactor parameters, and documentation of the results of the measurements. As such, these were the foundational documents for the LEU startup test plan described here. Julian and his associates at MURR measured the approach to critical, core void coefficient of reactivity, flux trap void coefficient of reactivity, determination of the reactivity worth of flux trap samples, thermal neutron mapping of the core, reactivity calibration of the control blades, primary and pool coolant temperature coefficients of reactivity, and flux distribution for experiments. While some aspects of the reactor have changed significantly since the Julian report (such as the graphite reflector and flux trap), the design of the HEU fuel elements evaluated in 1971 are the same as the fuel elements that are used today. NUREG-1537 requires that comparisons to HEU parameters be included in the startup test plan, where applicable. To accommodate this, comparisons of predicted LEU values to HEU are included in this chapter.

Similar to the analysis performed for the proposed LEU core at MURR in the current work, other USHPRR have completed analyses of startup tests. For example, analyses have been completed to verify the MITR LEU physics model, including predictions of several reactor physics parameters and comparisons to measured data for HEU [22]. NBSR has proposed a loading and startup test plan for cores following initial conversion to LEU [23]. Unlike MURR, NBSR will be initially loaded with a combination of HEU and LEU fuel elements, making their

test plan fundamentally different than the MURR test plan. The University of Massachusetts – Lowell Research Reactor also performed physics calculations in support of LEU fuel conversion in 2000 [24].

B. MODELING

In order to complete predictions for the various reactivity coefficients and flux mappings in support of the startup test plan, MCNP5 was used for eigenvalue calculations and neutron flux tallies. MCNP5 was also chosen for the ease of editing input files, particularly for temperature and density treatment.

While MURR uses MCNP5 frequently, its use is typically for calculations of experiment flux/fluence or critical control blade height predictions cycle-to-cycle. This model has the experiments modeled in detail, and updates to the model are made when the experiment loading of the reactor changes. However, for the startup test plan prediction analysis, MURR is assumed to be in a "clean core" state. That is, there will be no experiments present in the irradiation positions in the center flux trap or graphite reflector, and all reactor components (fuel, reflectors, and control blades) are assumed to have no irradiation history. Depending on the reactor parameter being analyzed, the center flux trap was modeled either with or without the six-barrel flux trap experiment holder. At the time of actual conversion, the startup test predictions will be either repeated or empirically adjusted to account for the effects of previous reflector and control blade operating history. Likewise, the effect of any changes to the experiment irradiation positions on the startup test predictions will need to be considered.

The temperature and pressure of the pool water and primary coolant and temperature of reactor components were modeled to best approximate the actual low-power startup test conditions. The bulk pool water temperature was assumed to be 38 °C, except when calculating the pool temperature coefficient of reactivity, in which case the pool temperature was assumed to vary from 32 °C to 54 °C. The primary coolant temperature was also assumed to be 38 °C during tests operating in natural convection mode, 54 °C when operating in forced flow conditions, and varied from 32 °C to 54 °C for cases when calculating the primary coolant temperature coefficient of reactivity. Both the pool and primary coolant water were modeled at 159 kPa during natural convection operation, and the primary coolant water was modeled at 414 kPa during forced flow operation. With the exception of the prediction of the flux mapping of the core, the startup physics tests will be performed at low power conditions (< 100 kW). Because of this, there will be little neutron and gamma heating of the core materials from fission. Consequently, the fuel and cladding can be assumed to be isothermal with the primary coolant while the beryllium and graphite reflectors can be assumed to be isothermal with the pool water. It is expected that the experimental position flux mapping test will be completed with the reactor at full power, and the temperature and pressure assumptions for the pool and primary coolant water will reflect that condition. Table V lists the reactor power, pressure, and temperatures assumptions for the LEU startup physics tests.

Case	Flux Trap Condition	Reactor Power	Primary Pressure (kPa)	Primary Coolant Temperature (°C)	Pool Water Temperature (°C)
Approach to Critical	Empty	0	159	38	38
Primary Coolant Void Coefficient	Empty	1 kW	159	38	38

Flux Trap Void Coefficient	Holder	1 kW	159	38	38
Flux Trap Sample Worth	Holder with Samples	1 kW	159	38	38
Axial and Radial Thermal Neutron Mapping	Holder	500 W	159	38	38
Control Blade Calibration	Holder	< 100 kW	414	54	38
Primary Coolant Temperature Coefficients	Holder	1 kW	414	Varies (32 to 54)	38
Pool Temperature Coefficient	Holder	1 kW	414	54	Varies (32 to 54)
Flux Mapping of Experimental Positions	Holder	12 MW	414	54	38

Table V: Reactor Conditions for LEU Low Power Physics Tests

C. RESULTS

Nine reactor physics parameters will be measured during the startup tests. Predictions were completed for all nine. These parameters are:

1. Approach to critical
2. Primary coolant void coefficient of reactivity
3. Flux trap void coefficient of reactivity
4. Reactivity worth of flux trap samples

5. Axial and radial distribution of the thermal neutron flux
6. Control blade calibration
7. Primary temperature coefficient of reactivity
8. Pool temperature coefficient of reactivity
9. Flux mapping of experiment positions

1) Approach to Critical

In order to accurately predict the critical loading of the initial LEU core, subcritical steps to criticality are necessary. To do this, a neutron source will be placed in the core and a baseline count rate, C_0, will be taken. As fuel is loaded into the core, the count rate will increase to a new value C_n, which can be predicted by the following equation:

$$C_n = C_0(1 + k_1 + k_2^2 + \cdots)$$

Because the higher order eigenvalues are much less than k_1, this equation can be simplified to:

$$C_n \approx \frac{C_0}{1 - k_{eff}} = C_0 M$$

As k_{eff} approaches 1.0, 1/M approaches zero. By plotting the subcritical count measurements, the 1/M plot can be extrapolated to zero, predicting the loading at which the reactor will become critical.

As a first prediction, the approach to critical was modeled in MCNP5. With the primary coolant and pool at natural convection temperature and pressure conditions and the control blades and regulating blade fully withdrawn, fuel elements were modeled one at a time to calculate the subcritical eigenvalue. Once the k_{eff} was predicted to be greater than 1.0, the critical

control blade heights were determined by analysis. For these cases, the regulating blade was positioned at mid-point of its withdrawal range, which is near the typical position during MURR operations. The results are summarized in Table VI.

Core Description	k_{eff}	Standard Dev.	Reg. Blade Height (cm)	Control Blade Height (cm)
1 Element Loaded	0.57945	0.00005	66.06	66.06
2 Elements Loaded	0.74718	0.00005	66.06	66.06
3 Elements Loaded	0.84142	0.00005	66.06	66.06
4 Elements Loaded	0.90296	0.00005	66.06	66.06
5 Elements Loaded	0.94773	0.00005	66.06	66.06
6 Elements Loaded	0.98566	0.00005	66.06	66.06
7 Elements Loaded	0.99995	0.00005	31.75	47.69
8 Elements Loaded	1.00003	0.00005	31.75	33.50

Table VI: Approach to Critical Results

As Table VI shows, MURR is predicted to be subcritical with less than seven fresh LEU elements loaded in the reactor core and the control blades fully withdrawn. MURR should achieve criticality with the insertion of a seventh fresh LEU element. For the full core loading of eight fresh LEU elements, no experiments in the center flux trap or graphite reflector, and no prior irradiation of the reactor components (e.g., control blades or beryllium reflector), it is predicted that MURR will achieve criticality with the control blades at 33.50 cm, and the regulating blade at 31.75 cm. This reactor configuration is the base model for the next startup test: the measurement of the coefficient of reactivity for primary coolant voiding.

2) Measurement of Core Void Coefficient of Reactivity

To prevent any positive reactivity insertion as a response to coolant voiding, MURR is designed to have a negative reactivity feedback in the event of primary coolant voiding, which is required by the MURR Technical Specifications to be more negative than -2×10^{-3} $\Delta k/k/\%$-void [25].

To begin this test, a baseline reactivity measurement will be taken with no experiments in the graphite reflector positions and no experiment holder in the center flux trap. It is expected that the primary coolant and pool conditions for this test will be under natural convection conditions. The control blade heights and the regulating blade height should be identical to the last approach to critical step, that is, 33.50 cm and 31.75 cm, respectively. Then, shims fabricated from AA6061 or similar material will be placed in the 22 interior coolant channels of one fresh LEU element to simulate a primary coolant void (Figure 5). It is assumed that the shims will measure 0.108 cm thick by 0.635 cm wide by 64.77 cm long and displace water equivalent to a primary coolant void of 0.435%. Because aluminum is essentially transparent to neutrons, and with an aluminum concentration in the AA6061 greater than 95 weight percent, the shims will be an effective replacement for an actual air void in the primary coolant channels [26]. In addition to shims in all interior coolant channels, a reactivity measurement will be taken with shims in the even numbered coolant channels as another point of comparison. In this case, the effective coolant void fraction from the shims is 0.218%.

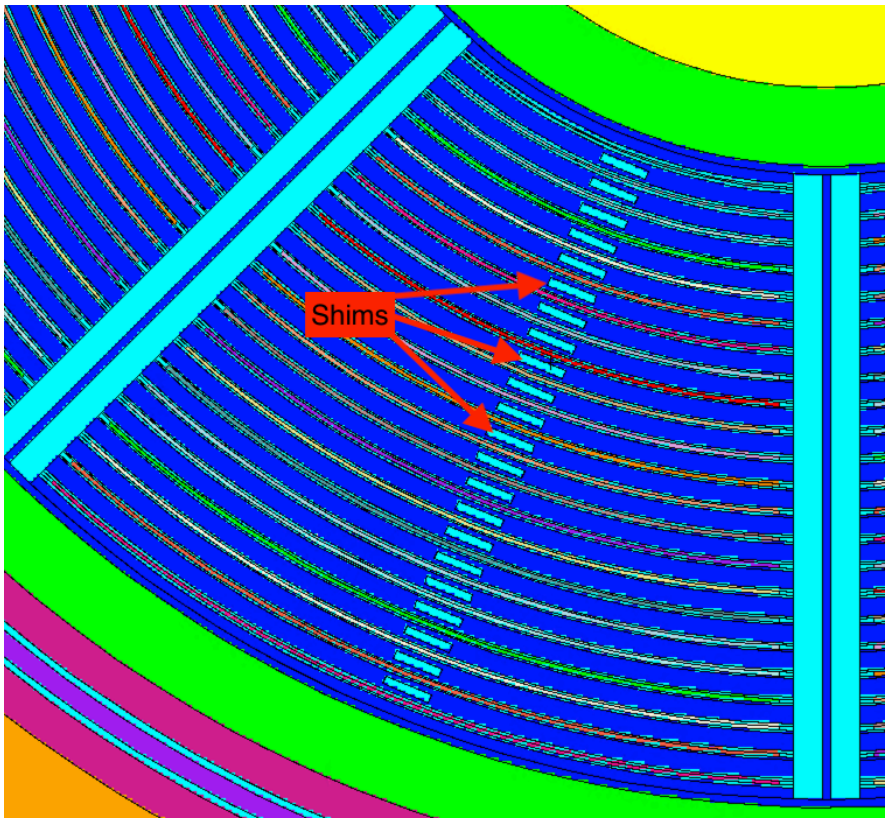

Figure 5: Shims in Interior Coolant Channels of MURR LEU Fuel Element

Several cases were run to complete predictions for this startup test. The results of all predictions are presented in Table VII. First, the baseline case with eight fresh LEU elements containing no shims was run. The control blades were positioned at 33.50 cm and the regulating blade was at 31.75 cm withdrawn. The k_{eff} for this case was calculated as 1.00008±0.00005, which is within one standard deviation of the results for the similar case reported in Table VI. Next, shims with the same dimensions as expected for the startup test (described above) were modeled in all of the interior coolant channels of the fresh fuel element in core position X8. The shims were assumed to be fabricated from AA6061 with an equivalent boron content (EBC) of 10 parts per million (ppm) to account for impurities in the aluminum alloy. A case with shims positioned only in the even numbered coolant channels was also run. With shims in all the

interior coolant channels, the best-estimate void coefficient of reactivity predicted by MCNP5 for the core loaded with fresh LEU fuel elements is -3.13×10^{-3} Δk/k/%-void. Based on the relative error of the MCNP5 analyses, the 2-σ standard deviation of this predicted value is 0.32×10^{-3}. For the core loaded with fresh HEU fuel elements, the measured value of the coolant void coefficient was -3.08×10^{-3} Δk/k/%-void [21] which is within one standard deviation of the calculated value for LEU. This indicates that there is no statistically significant difference between the predicted coolant void coefficient for LEU relative to the current HEU fuel. For the case with shims in the even numbered coolant channels of the HEU element, MURR observed a void coefficient of -2.965×10^{-3} Δk/k/%-void. For the comparable case with LEU, the magnitude of the void coefficient is predicted to be 8.6% lower, but is again within the statistical uncertainty of the calculation.

Description	k_{eff}	Std. Dev.	Percent void	Δk/k (10^{-3})	Δk/k/%-void (10^{-3})	Std. Dev. (10^{-3})
No shims baseline	1.00008	0.00005	0	0	0	0
Shims in all coolant channels (10 ppm EBC)	0.99872	0.00005	0.435	-1.36	-3.13	0.16
Shims in even coolant channels (10 ppm EBC)	0.99949	0.00005	0.218	-0.590	-2.71	0.32
Shims in all coolant channels (20 ppm EBC)	0.99880	0.00005	0.435	-1.28	-2.95	0.16

Description	k_{eff}	Std. Dev.	Percent void	$\Delta k/k$ (10^{-3})	$\Delta k/k$/%-void (10^{-3})	Std. Dev. (10^{-3})
Void replaces shims in all coolant channels	0.99877	0.00005	0.435	-1.31	-3.01	0.16

Table VII: Void Coefficient of Reactivity Cases

Because of the importance of this startup test, two branch cases were also modeled for the prediction analysis to understand the impact of the material used to model the shims and to understand any bias between the measured reactivity worth from the aluminum shims and the reactivity worth of a void in the coolant. In the first branch case the EBC in the AA6061 shims was increased in the model from 10 to 20 ppm. Since the boron (or boron equivalence) in the shims has a high neutron capture cross-section, this variation could potentially impact the void coefficient measurement. In the second branch case, a pure void (zero neutron importance) was modeled in MCNP5 in cells with the same dimensions as the shims. In both cases, the predicted coolant void coefficient is statistically the same (within one standard deviation) as the case with 10 ppm boron in the shims, indicating that there is expected to be a negligible impact from the EBC of the AA6061 used to manufacture the shims for this startup test.

In the HEU startup test report, a reduction factor was applied to the measured aluminum shim void coefficient to account for neutron absorption in the shims to calculate the true void coefficient relative to the case of an actual void in the coolant. This reduction factor was estimated as 17% based on the aluminum absorption cross section. The calculated results presented in Table VII show that the predicted void coefficient for the pure void case and that calculated with aluminum shims are all within 10% (two standard deviations) of one another. Potentially, a follow-up test could be a void reactivity coefficient measurement with hollow

aluminum shims to examine whether there is an observed difference between aluminum and a void reactivity worth.

For all reactor physics measurements performed for the HEU core, the average reactivity coefficient was observed value to be -3.02×10^{-3} Δk/k/%-void. The average of the four MCNP5 simulations for the LEU coefficient of reactivity was 2.3% lower in magnitude, or -2.95×10^{-3} Δk/k/%-void. The relatively close agreement between the HEU and LEU values lend confidence to the predicted LEU values.

The true importance of this startup test is to confirm that with the LEU fuel elements loaded in the core following conversion, MURR will be within its operating requirement that the void coefficient of reactivity be more negative than -2×10^{-3} Δk/k/%-void. These predictions show that the technical specification is met with the LEU fuel. However, because of the importance of demonstrating compliance with the technical specification limit, care should be taken not only in this startup test, but also in precisely calculating the control blade worth curves that will be used to derive the void coefficient. Modeling could also be helpful in providing additional support to the experimental value should both the model and experiment agree in their calculated void coefficient values.

3) Void Coefficient of the Flux Trap Region

While MURR has a negative primary coolant void coefficient of reactivity, voiding in the flux trap region introduces a positive reactivity insertion. The flux trap region is the space inside the annular ring of fuel elements in the core. The water that fills the flux trap is outside the inner

pressure vessel, and as such its temperature and pressure properties are the same as the bulk pool water. In order to experimentally represent voiding of the pool water in the flux trap, the six-tube experiment holder will be installed in the flux trap. To simulate flux trap voiding, air-filled aluminum cans that are 10.16 cm long and with 0.0762 cm thick walls will be used in Tube A of the flux trap experiment holder. This is shown in Figure 6.

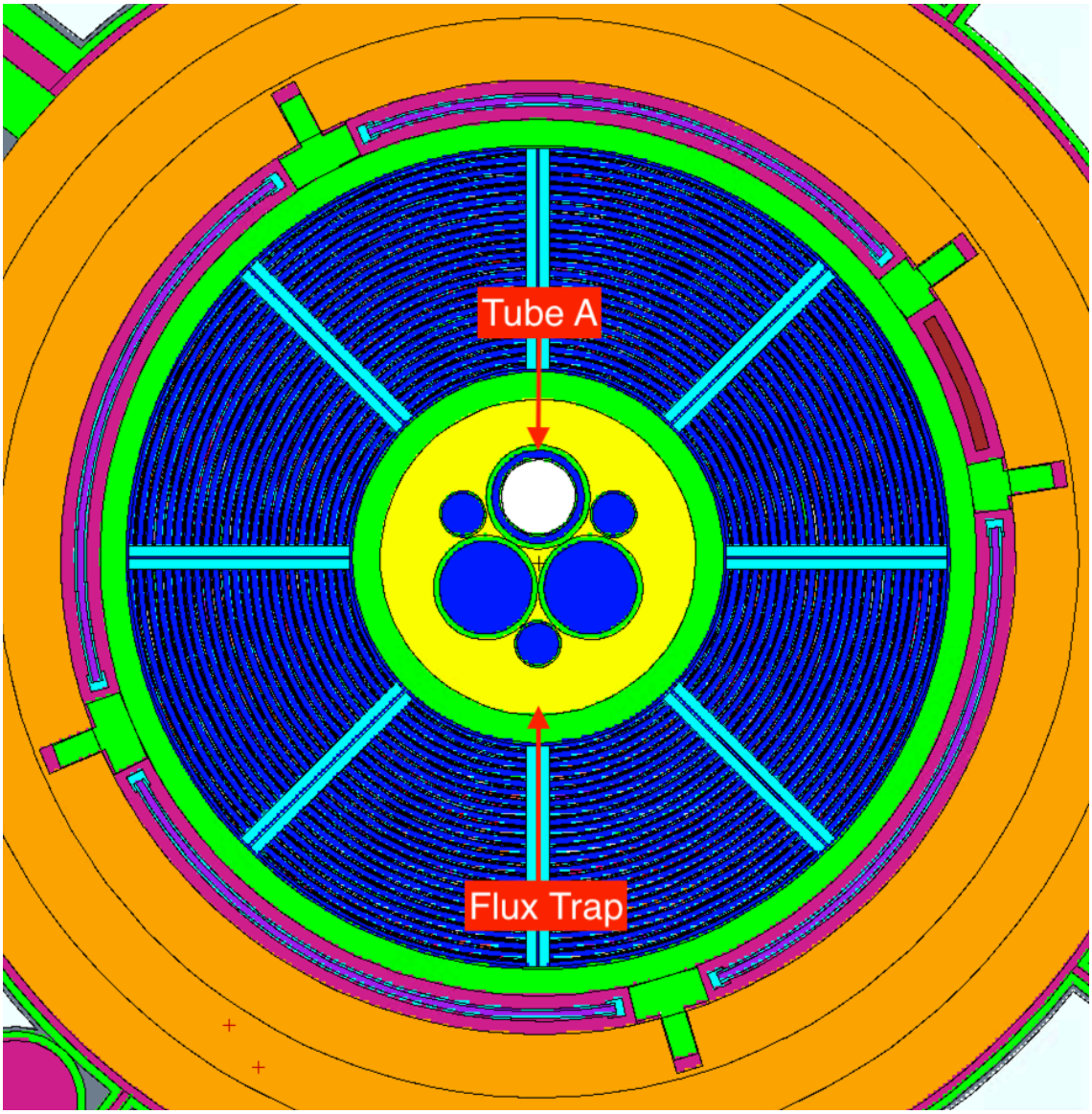

Figure 6: Center Flux Trap Region for Flux Trap Voiding

During the test, a baseline reactivity calculation will be done with the six-tube experiment holder with no cans in Tube A. The critical control blades positions for this configuration was the four BORAL control blades at 32.494 cm and the regulating blade at 31.75 cm. The primary coolant and pool water will be at natural convection temperature and pressure conditions. Then, the air-filled cans, two at a time, will be progressively stacked on top of one another, starting at the bottom of the experiment holder, until the full 81.28 cm length of Tube A is filled with voided cans. In total, five reactivity tests will be done to effectively measure the flux trap void coefficient. The reactivity worth of the void will be determined in the same way as in the primary coolant void coefficient test; that is, using the change in the critical control blade position and the integral blade worth to determine the change in core reactivity. Reactivity change as a function of percent void can then be calculated, yielding the flux trap void coefficient of reactivity.

To predict the flux trap void coefficient, MCNP5 was again used to model the startup test in detail. It was assumed that the water displaced by the entire can (65.2 cm^3) should be included in the void volume. This assumption, much like the primary void coefficient cases before, is based on the small neutron cross-section of aluminum. Thus, the true void is represented by taking the can as a whole into consideration, not just the void inside the can. All five cases were analyzed, and the results are summarized in Table VIII.

Description	Volume of water displaced	k_{eff}	Std. Dev.	$\Delta k/k$ (10^{-5})	$\Delta k/k/cm^3$-void (10^{-5})	Std. Dev. (10^{-5})
Empty sample holder	0	1.00007	0.00005	0	0	0
Void 0-20.32 cm	130.31	1.00070	0.00005	63.0	0.483	0.050
Void 0-40.64 cm	260.62	1.00375	0.00005	367	1.41	0.027
Void 0-60.96 cm	390.94	1.00490	0.00005	481	1.23	0.018

Description	Volume of water displaced	k_{eff}	Std. Dev.	$\Delta k/k$ (10^{-5})	$\Delta k/k/cm^3$-void (10^{-5})	Std. Dev. (10^{-5})
Void 0-81.28 cm	521.25	1.00485	0.00005	476	0.913	0.013

Table VIII: Flux Trap Void Coefficient of Reactivity Cases

A comparison of the flux trap void coefficient of reactivity measured for the all-fresh HEU core and predicted by analysis for the all-fresh LEU core is provided in Figure 7, with 2σ uncertainty for the LEU values. It can be seen that the predicted flux trap void coefficient for the LEU core is larger (more positive) than the flux trap void coefficient measured for the HEU core in 1971. However, the predicted LEU values do follow the same general trend as the measured HEU values, with a maximum value reached when the void is introduced in the axial midplane of the core and a smaller reactivity change for a given void volume at the top and bottom of the core. This seems likely due to the shape of the neutron flux of the core and flux trap region, which peaks near the core midplane and decreases near the top and bottom of the core. Because of the relatively lower neutron populations at the top and bottom of the core, there is a corresponding lower reactivity effect from voiding in the flux trap near the top and bottom of the core. Further supporting this conclusion is the negligible change in the k_{eff} value when the void is added near the top of the flux trap. The relative effect of additional voiding is negligible because of the lower neutron importance in this axial region of the core.

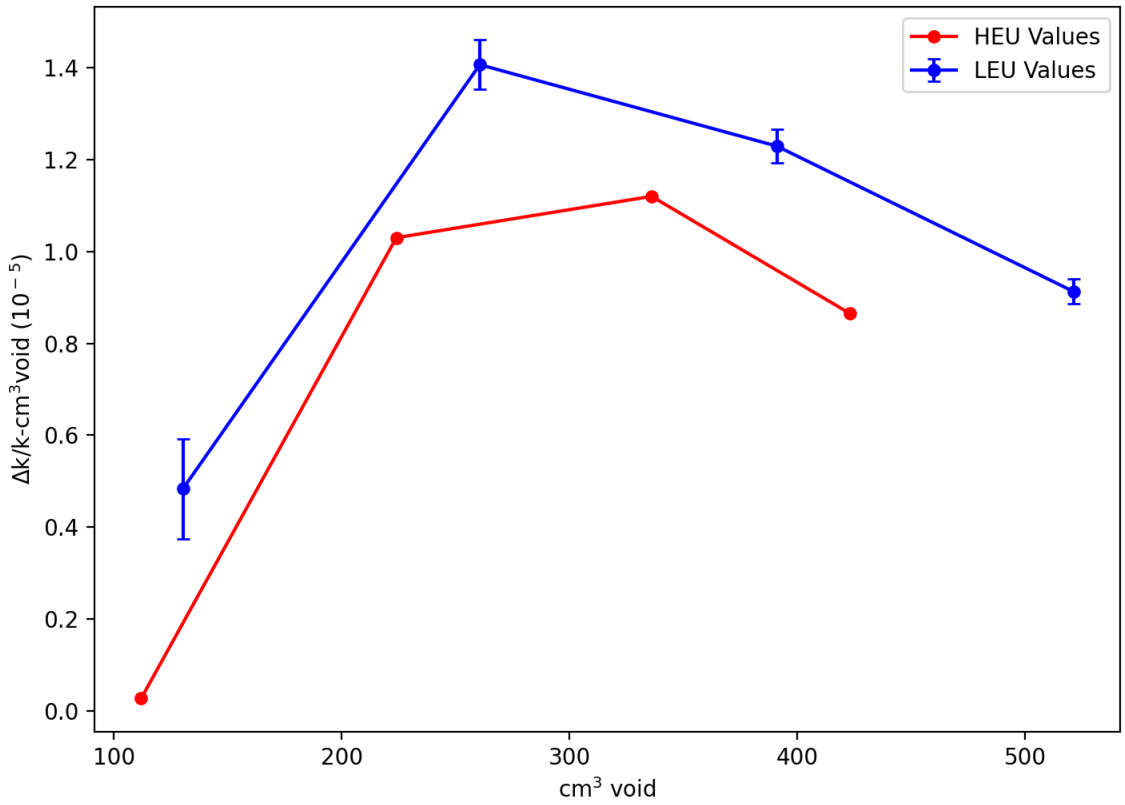

Figure 7: Comparison of HEU and LEU Flux Trap Void Coefficients of Reactivity

4) Determination of Reactivity Worth of Flux Trap Samples

As established in Section 3, the flux trap region of MURR is an area with high sensitivity to hardware additions, voids, and other perturbations, especially in the axial center of the fueled region. Because of this, it is important that MURR establish some baseline for reactivity worth of common flux trap samples. Flux trap samples are housed in the six-barrel experiment holder, shown in Figure 6. The samples are typically placed in aluminum cans, ranging from 5.08 cm to 10.16 cm long. MURR allows for a variety of materials to be irradiated in the flux trap region, making it impractical to complete precise reactivity predictions for experiments when MURR

converts to the use of LEU fuel several years in the future. However, some samples that are irradiated currently have a long history of irradiation at MURR and may be used well into the future. Consequently, these samples were chosen to be representative for reactivity determination predictions.

Three typical sample materials irradiated in the flux trap were chosen for reactivity measurement predictions: molybdenum, titanium, and TheraSphere^{TM}. Irradiation of molybdenum produces molybdenum-99 by an (n,γ) metal reaction. ^{99}Mo has a 66-hour half-life and decays by beta emission to ^{99m}Tc ($t_{1/2}$ = 6 hr), which is a highly sought-after medical isotope for diagnostic and imaging functions [27]. Titanium is the standard material used for reactivity hold down to meet MURR's Technical Specifications requirement that the maximum reactivity for center flux trap experiments not exceed 0.006 Δk/k [25]. TheraSphere [28] is a radiopharmaceutical product that has been produced at MURR for many years, in collaboration with Boston Scientific, for the treatment of liver cancer. The TheraSphere product consists of glass microspheres containing ^{90}Y, a beta emitter with an average decay energy of 0.9367 MeV. All three samples have a long history of irradiation at MURR.

During this startup test, a baseline reactivity case of an empty six-tube experiment holder will be taken, with the control blade positions at the same heights as in Section 3. The primary coolant and pool water will be at the temperature and pressure of natural convection. As in the flux trap void coefficient of reactivity cases, Tube A of the experiment holder will be used to hold the samples. To space the samples appropriately, Tube A will be filled with water-filled aluminum cans and a reactivity measurement will be taken. Next, 4-inch long (10.16 cm) sample cans containing either molybdenum, titanium, or TheraSpheres will be inserted in Tube A, with the tops of the cans at the axial midplane of core, and reactivity measurements will be taken for

each sample. Finally, three 4-inch cans containing molybdenum will be inserted into the three large diameter tubes (Tubes A, B, and C), and a reactivity measurement will be taken. These cases were modeled in MCNP5, and the predicted reactivity worth of the various samples are documented in Table IX.

Description	k_{eff}	Std. Dev.	$\Delta k/k$ (10^{-3})	Std. Dev. (10^{-3})
Empty Flux Trap	0.99585	0.00005	-4.24	0.07
Empty sample holder	1.00007	0.00005	0	0
Flux trap with water-filled cans in Tube A	1.00068	0.00005	0.610	0.07
Molybdenum Sample in Tube A	0.99859	0.00005	-1.48	0.07
Titanium Spacer in Tube A	0.99761	0.00005	-2.47	0.07
TheraSphere sample in Tube A	1.00124	0.00005	1.17	0.07
Molybdenum Sample in Tubes A, B, C	0.99670	0.00005	-3.38	0.07

Table IX: Determination of Flux Trap Samples Cases

These samples have a non-negligible impact on the reactivity of the reactor. This analysis confirms that titanium spacers in the center flux trap are effective for reactivity hold down. Likewise, the molybdenum samples introduce a substantial amount of negative reactivity. Other samples, which were not modeled in this analysis, will generally introduce positive reactivity due to the displacement of water in the center flux trap. In total, the reactivity worth of all experiments typically loaded in the center flux trap is approximately $+6\times10^{-3}$ $\Delta k/k$, which is the MURR Technical Specification limit.

For comparison, during the HEU startup test, MURR also tested a natural molybdenum target in the flux trap and determined the reactivity change to be -2.84×10^{-4} $\Delta k/k$. The exact

configuration of the 1971 experiment was not preserved and thus it cannot be confirmed whether the molybdenum sample modeled for this analysis is like-for-like. Nevertheless, the small change in reactivity worth is an important determination for confidence in continued flux trap irradiations at MURR.

5) Radial and Axial Thermal Neutron Mapping of the Core

Determining the thermal neutron flux profile of the new LEU core is key for experimenters and modelers alike. Many experiments at MURR rely on activation by thermal neutrons, and where experiments should be positioned to get the necessary flux or fluence is determined by the thermal neutron flux profile. During typical HEU operation, MURR has an axial flux profile that is peaked slightly below the axial midplane of the core and lower towards the bottom and top of the fuel. When the initial all-fresh LEU core is loaded in MURR, the shape of the flux will be perturbed by the deeper insertion of the control blades. This perturbation is expected to be most pronounced closer to the outer radius of the core, but because the blades are much more deeply inserted than during typical mixed-core burnup operation, it is likely that the flux will be altered even in the inner fuel channels and flux trap.

To determine the thermal flux profile, pure gold wires 0.0254 cm in diameter will be attached to the aluminum shims that are used to test the coolant void coefficient of reactivity. These wires will run the full length of the fuel. The reactor will be operated at critical for one hour at 500 watts at the water conditions present during the primary coolant void coefficient of reactivity measurement, after which the wires will be allowed to decay for a determined length of time before being divided into one-inch segments for activation analysis. Gold has a significant

(n,γ) thermal (E < 1 eV) neutron capture cross-section, ranging from approximately 4000 barns at very low neutron energies to 25 barns at 1 eV. This neutron capture cross-section is large enough to have a meaningful amount of neutron capture to provide adequate counting statistics, but low enough that the gold will not burn out during irradiation. The gold wires were modeled in MCNP5 as attached to the 22 aluminum shims inserted in each of the coolant channels between fuel plates. The wires were divided into 24 one-inch segments in a f4 flux tally to obtain the predicted axial and radial thermal flux profile for the all-fresh LEU core.

Figure 8 shows the predicted peak-to-average ratio of the thermal flux for each coolant channel in the LEU fuel element in core position X8 of the all-fresh LEU core. The peak-to-average ratios predicted for the LEU core compare favorably with the peak-to-average ratios measured during the HEU startup test. Channel 2 (between plates 1 and 2) is predicted to have a peak-to-average ratio of 1.44 for the fresh LEU fuel element, while the fresh HEU fuel element peak-to-average value for the same channel (identified as channel 1 in the HEU report) was predicted by analysis to be 1.43 and measured during the startup test as 1.45.

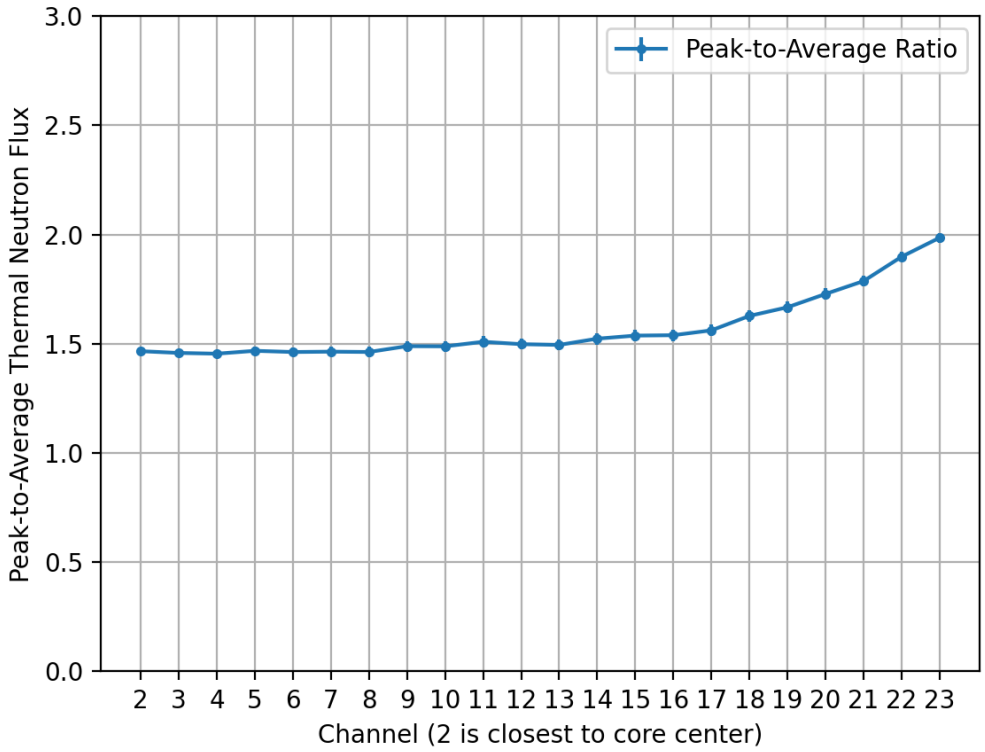

Figure 8: Peak-to-Average Ratio of the Thermal Neutron Flux in Fresh LEU Element

The results presented in Figure 8 show that the peak-to-average thermal flux is relatively constant in channels 2-17 but increases for the outermost radial channels, reaching a value of 1.99 for channel 23 (between plates 22 and 23). The outer channels are closest to the control blades, which have a greater effect on the axial flux profile and cause the increase in the peak-to-average flux in these coolant channels.

Figure 9 shows the average and maximum thermal flux in each coolant channel of the fresh LEU element. The flux was normalized to a total reactor power of 500 W. As expected, the magnitude of the thermal flux is greater in the innermost and outermost coolant channels due to the effects of the center flux trap and the beryllium reflector, respectively, and lowest in the channels that are near the center of the element due to self-shielding effects. The maximum radial peaking factor for the channel average thermal neutron flux in the fresh LEU fuel element

was predicted to be 2.55 in coolant channel 2, compared to a measured radial peaking factor of 2.23 for the fresh HEU fuel element. It should be noted that the LEU fuel element is designed with the thinnest fuel cores in those plates that are closest to the center flux trap to reduce the radial peaking.

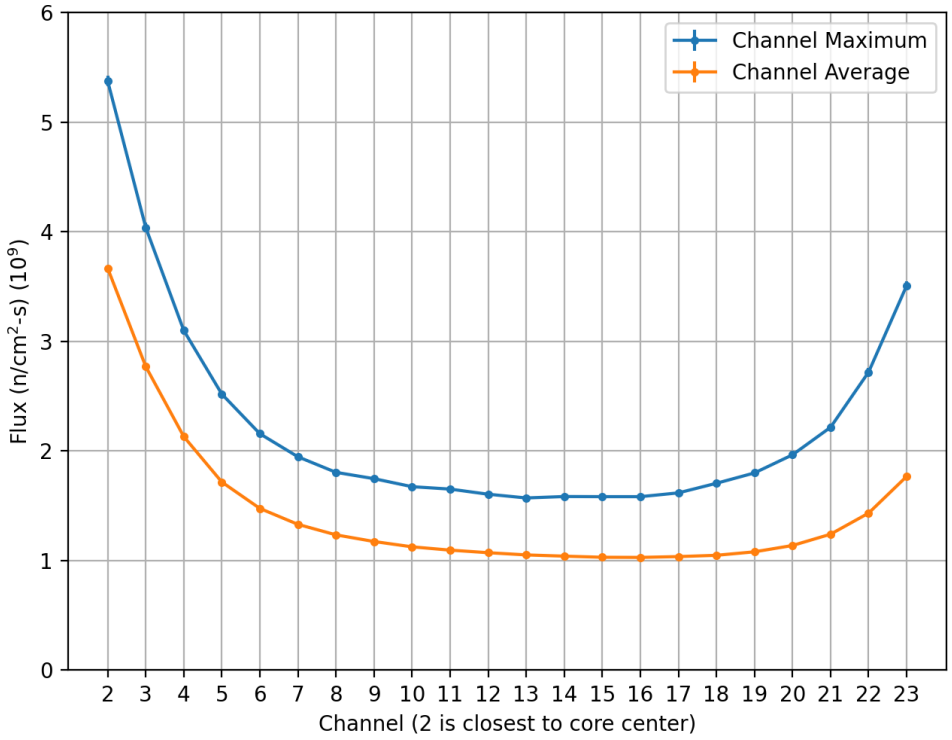

Figure 9: Average and Maximum Thermal Flux in Coolant Channels in Fresh LEU Element

Figure 10 shows the axial distribution of the predicted thermal neutron flux in three coolant channels of the fresh LEU fuel element. Channel 2 is located between plates 1 and 2 near the center flux trap, channel 15 is an interior channel between plates 14 and 15, and channel 23 is between plates 22 and 23 near the control blades and beryllium reflector. All three channels show the same general axial profile, with the largest thermal flux at approximately 15.24 cm (6 in) from the bottom of the fuel. The flux is lower in the upper part of the core than the bottom of the core due to the influence of the control blades. The effect of the control blades on the axial

flux profile can be especially seen for channel 23, which has a much larger peak-to-average thermal neutron flux.

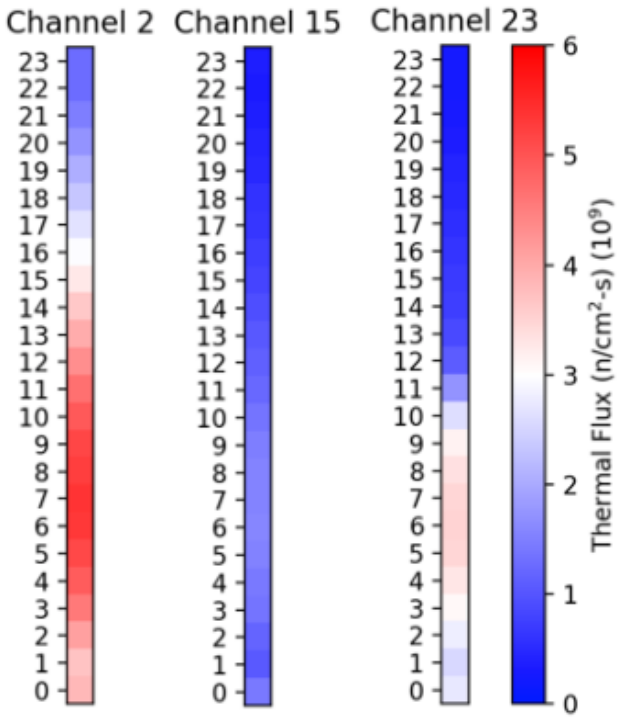

Figure 10: Axial Thermal Flux Distribution in Channels 2, 15, and 23

6) Reactivity Calibration of the Control Blades

During the startup tests, the determination of the reactivity worth for all reactor physics measurements will be derived using the integral and differential worth of the control blades. MURR's primary reactivity control is from the four BORAL control blades that are located in a channel between the outer reactor pressure vessel wall and the beryllium reflector. There is also a stainless-steel regulating blade for fine reactivity control. The blades are inserted from the top of the reactor and are withdrawn to compensate for reactivity changes in the reactor. The withdrawn

position of the control blades is identified as the distance from the tip of the BORAL material in the blades and a position one inch below the bottom of the fuel plates. The blades travel 66.04 cm vertically. Each of the control blades and the regulating blade are identified in Figure 11.

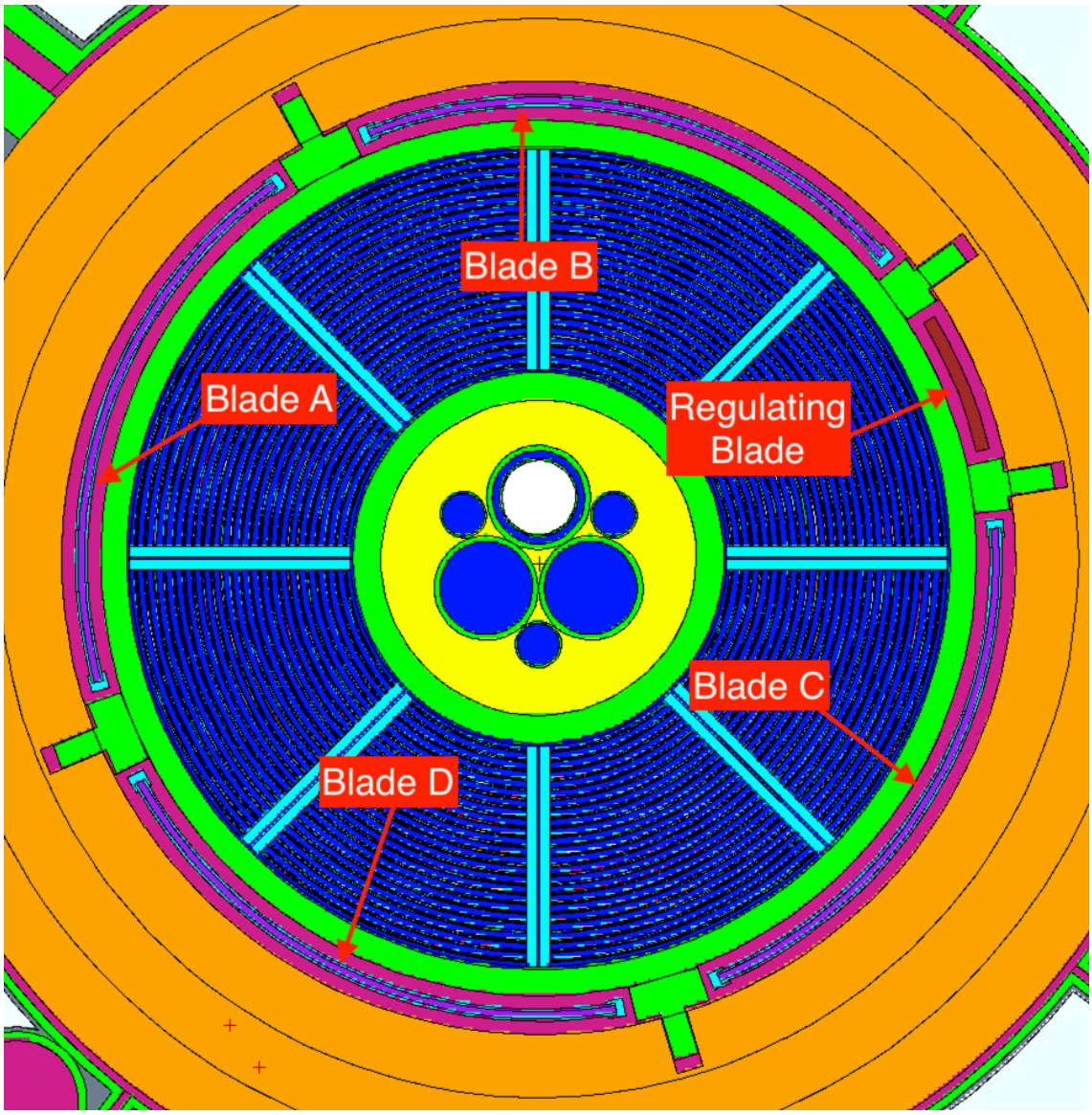

Figure 11: Control Blades in MURR Core

A key difference between the prediction analysis and the actual startup test is the method by which reactivity worth is calculated. For the prediction analysis, reactivity worth is calculated using the following eigenvalue equation:

$$\Delta\rho = \frac{k_2 - k_1}{k_1 k_2}$$

where k_1 and k_2 are the eigenvalues for the cases studied. During the startup test, the reactivity worth of the of the control blades will be derived by counting the neutron population doubling time using the following equation:

$$\Delta\rho = \frac{\ell}{T + \ell} + \frac{\ell}{T + \ell} \sum_{i=1}^{6} \frac{\beta_i}{1 + T\lambda_i}$$

Where ℓ is the mean neutron lifetime, T is the stable reactor period, and the summation is the typical six-group delayed neutron term. In practice, the reactor operators will bring the reactor into a critical configuration by adjusting the position of the control blades. Then, one of the control blades will be slightly withdrawn, making the reactor supercritical. By determining the stable reactor period of the supercritical state, the reactivity insertion can be determined and plotted on the blade worth curve.

At the time of the startup tests measuring the control blade reactivity worth, the control blades and beryllium reflector will have some prior operating history. Prior use of the control blades reduces the concentration of the ^{10}B in the BORAL material, particularly near the tip of the control blade, reducing their reactivity worth. Prior use of the beryllium reflector reduces its effectiveness as a neutron reflector, which causes a decrease in the core reactivity. Both of these reactor components are routinely replaced. At this time, it is not possible to predict what the conditions of these components will be at the time of conversion. Thus, for the current prediction analysis it was assumed that the four control blades and the beryllium reflector were at fresh conditions (no prior operating history). At the time of the startup tests, the predictions can be

repeated with the control blades and beryllium modeled at appropriate conditions or empirically adjusted to account for the effects of previous control blade and reflector operating history.

The predictions of the control blade worth were completed using an MCNP5 model with three of the control blades held at a constant height of 32.494 cm and the regulating blade at 31.75 cm, while the other blade traveled from 0 cm to 66.04 cm in 0.5 cm increments. The primary coolant system and pool were assumed to be at forced flow temperatures and pressures. Also, it was assumed that there were no experiments inserted in the experiment holder in the center flux trap and no experiments in the graphite reflector. The core eigenvalue was calculated with a sufficient number of histories to obtain a relative error of 0.00005 and was used to determine the reactivity worth relative to the blade fully inserted position. Both the integral and differential blade worth were calculated and are presented in Figure 12 and Figure 13. As expected, the differential reactivity worth of the control blades is greatest near the center of the core where neutron importance is the highest and decreasingly effective near the top and bottom of the core.

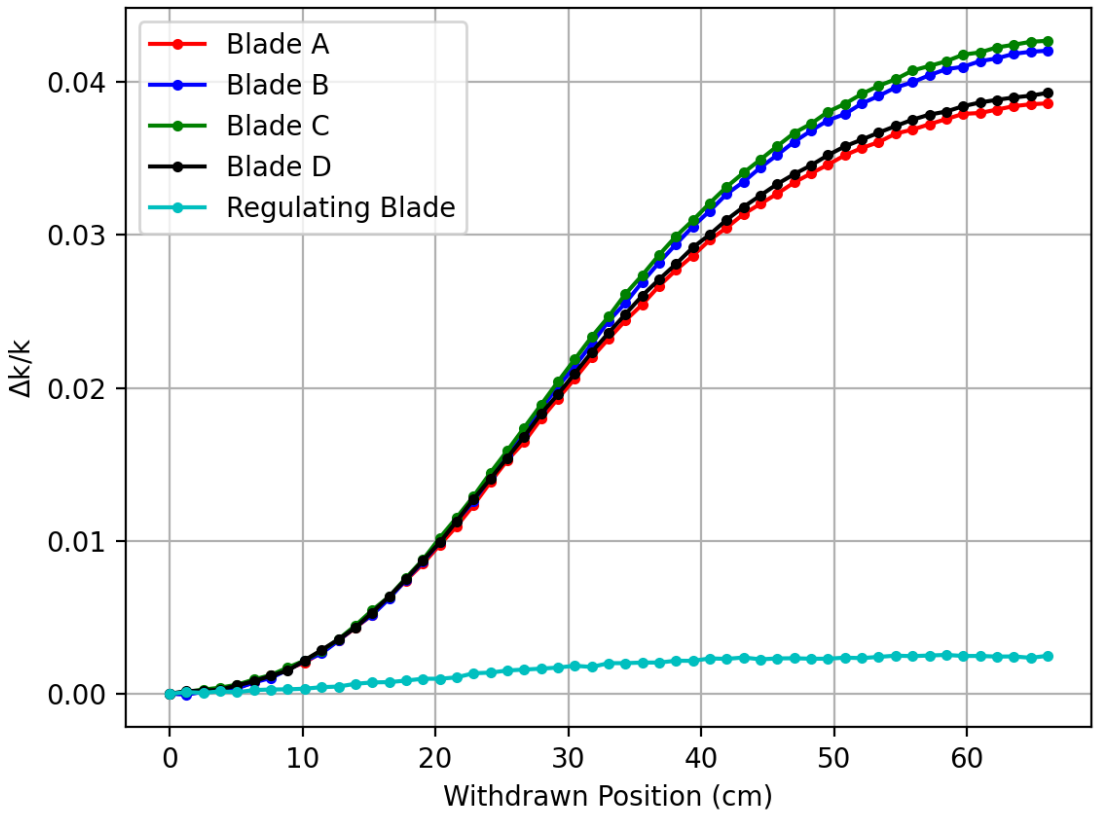

Figure 12: Predicted Integral Blade Worth for Fresh LEU Core

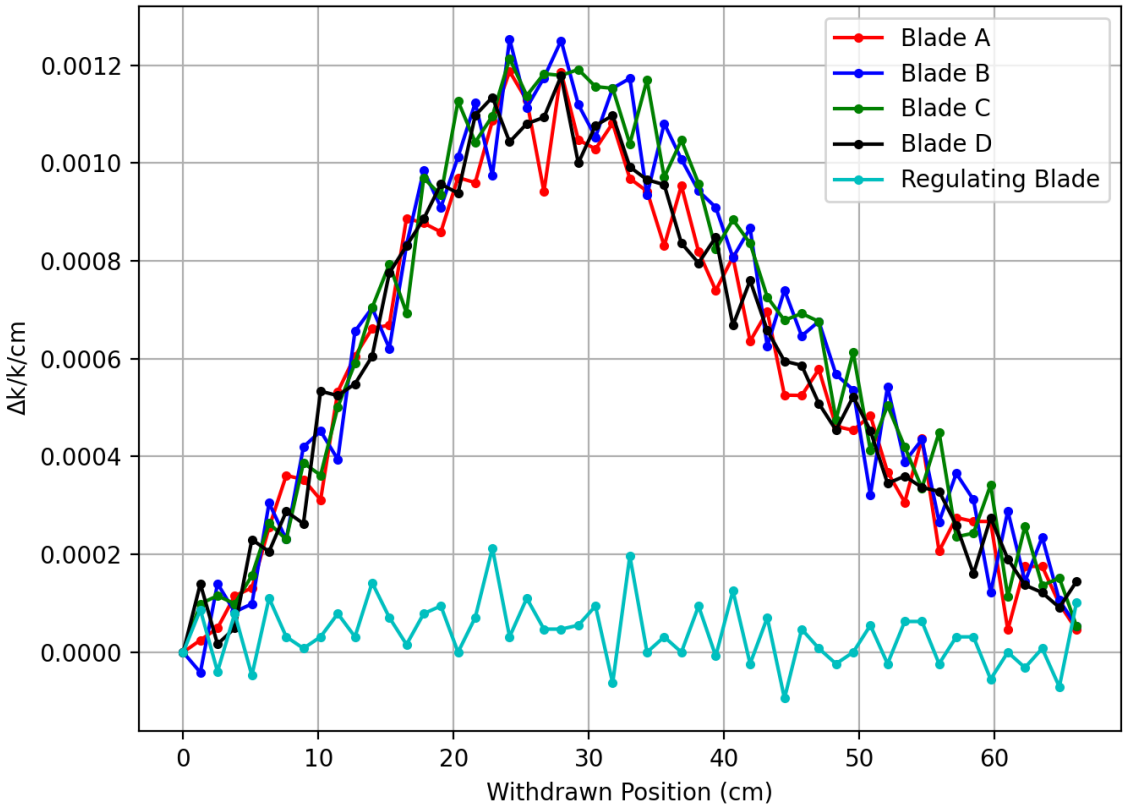

Figure 13: Predicted Differential Blade Worth for Fresh LEU Core

Also noticeable is the substantial "noise" in the predicted differential blade worth, which is partly due to the statistical uncertainty of the MCNP5 calculations. It is helpful to observe how this uncertainty may influence the differential blade worth curve. Figure 14 shows the predicted differential worth for Blade A and the regulating blade along with the 2σ uncertainty (95% confidence) for each. The true expected value for the differential blade worth should be somewhere within the red or green shaded bands in Figure 14. For instance, the maximum predicted differential worth of blade A is 0.00119 ± 0.00012 Δk/k/cm to 2σ uncertainty.

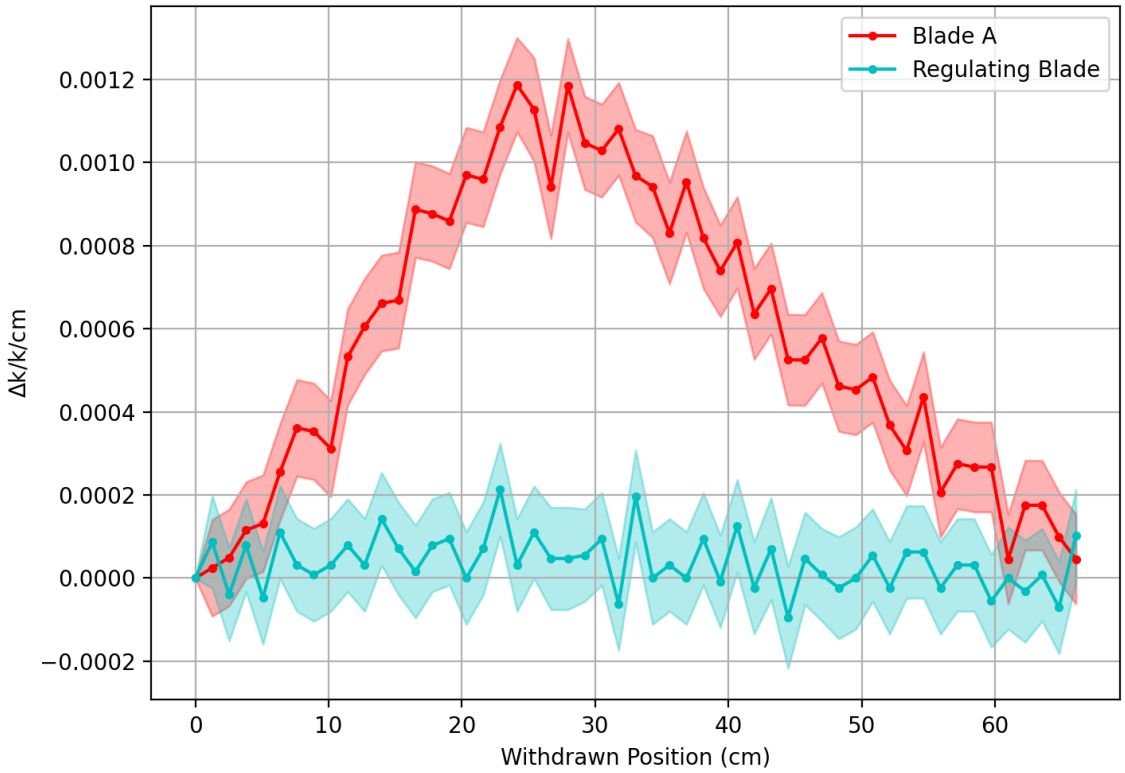

Figure 14: Differential Blade Worth Uncertainty of the LEU Core

By using the uncertainty of the differential worth of the control blades, the values used to generate Figure 13 can also be used to predict whether a Technical Specification requirement on the maximum reactivity insertion rate from blade withdrawal will be met. With the four control blades operating simultaneously, the rate of reactivity insertion cannot exceed 3.0×10^{-4} Δk/k/sec. Among all the control blades, the maximum differential blade worth is predicted to be 0.00125 ± 0.00012 Δk/k/cm with 2σ uncertainty (for blade B). The maximum rate of withdrawal of the control blades is 2.54 cm/min. Assuming all four control blades insert the maximum amount of differential activity plus 2σ uncertainty, the reactivity insertion rate is 2.32×10^{-4} Δk/k/sec, which satisfies the Technical Specification requirement.

The integral blade worth can be used to predict the "cold" shutdown margin, which is another key Technical Specification. According to the Technical Specification, the shutdown

margin shall be at least 0.02 Δk/k with the most reactive control blade and regulating blade fully withdrawn, irradiation facilities and experiments in their most reactive state, and the core at ambient temperature conditions with negligible xenon worth. While the experiments are not installed in the core used to generate the integral blade worth, the excess reactivity of the all-fresh LEU core loaded with samples that are typical for MURR's weekly operating cycle and at cold conditions was calculated to be 0.078 Δk/k. The results calculated for the integral reactivity worth of blades A, B, and D (the three lowest worth blades, as shown in Figure 12) were summed to obtain a total reactivity worth of 0.1200 ± 0.00024 Δk/k at 2σ uncertainty. Subtracting the lower bound of these blades (0.1197 Δk/k) from the cold excess reactivity results in an estimated cold shutdown margin of 0.0417 Δk/k, which is well above the Technical Specification value of 0.02 Δk/k.

However, summing the individual integral blade worth for the control blades may not be a conservative method of calculating the cold shutdown margin because of "shadowing" effects which can occur when the blades are fully inserted collectively. To provide a more accurate calculation of the cold shutdown margin, two branch cases were run. First, the cold excess reactivity for the all-fresh LEU core was calculated using MCNP5 with all control blades fully withdrawn and the core in cold, low-power conditions. For this calculation, typical experiment loadings were present in the graphite reflector and the center flux trap. The reactivity of this core configuration was determined to be 0.07802 ± 0.00008 Δk/k. To find the worth of the three least reactive blades, blades A, B, and D were fully inserted with blade C and the regulating blade fully withdrawn. The worth of blades A, B, and D inserted as a bank is calculated to be 0.10853 ± 0.00014 Δk/k, compared to 0.1200 ± 0.00024 Δk/k when the worth of the individual blades is added together. By subtracting the bank worth of blades A, B, and D from the excess reactivity,

the cold shutdown margin was determined to be 0.03051 ± 0.00010 Δk/k, which meets the Technical Specification requirement.

The second branch case studied was a more conservative case than the previous branch case. In this case, the fuel was fresh LEU, but no experiment holder was present in the center flux trap and the penetrations in the graphite reflector were water-filled (without experiments). The cold excess reactivity for this case was calculated as above and was found to be 0.07151 ± 0.00008 Δk/k. Adding the maximum allowed experiment worth in the center flux trap of 0.006 Δk/k and the experiment holder worth of 0.00424 ± 0.00014 Δk/k, the excess reactivity was determined to be 0.08175 ± 0.00016 Δk/k. Then, the reactivity worth of blades A, B, and D were calculated as before, and this value was determined to be 0.11048 ± 0.00014 Δk/k. Subtracting bank blade worth from the excess reactivity, the cold shutdown margin for this case was calculated to be 0.02873 ± 0.00018 Δk/k. This meets the Technical Specification requirement. It should be noted that any prior operating history on the control blades and the beryllium reflector, which are assumed to be fresh in this analysis, will impact the cold excess reactivity and shutdown margin, so these will be evaluated at the time of the startup tests. Likewise, the effect of changes to the experimental facilities relative to what has been modeled in the current analysis will need to be evaluated at the time of conversion.

Lastly, it is noted that the control blade worth curves, perhaps of all the tests, will be most helpful in validating the MURR LEU MCNP5 models. Biases in critical control blade positions should be apparent, and uncertainties in the model could be reduced by this validation study. The measurement uncertainties can be difficult to quantify and having a clean core with the least amount of uncertainty possible during initial operation will provide extremely useful information for completing rigorous validation of the MURR MCNP5 model.

7) Evaluation of the Primary and Pool Coolant Temperature Coefficients of Reactivity

The temperatures of reactor components at MURR are controlled mainly by two systems: the primary coolant water and the bulk pool water. The primary coolant water is the water inside the reactor pressure vessel and normally cools the fuel elements via forced convection. The water in the reactor pool cools experiments and other reactor components also by forced circulation. As heat is added to the primary coolant water during steady-state reactor operations and transient conditions, the corresponding decrease of the water density causes a decrease of the core reactivity due to the negative primary coolant void feedback coefficient of reactivity (see Section 2). On the other hand, as the temperature of the pool water increases, the density of the water in the flux trap decreases, causing a reactivity increase due to the positive flux trap void coefficient (see Section 3).

The startup tests described in Sections 2 and 3 are used to determine the reactivity change due to water density changes only. The startup tests of the primary and pool coolant temperature coefficients described in this section will quantify the reactivity change from temperature changes which affect not only water density but also the water scattering properties.

The primary and pool coolant temperature coefficients of reactivity will be tested separately. The primary coolant system will be tested first. MURR operators will bring the reactor critical to a power level of 1 kW, using pumps to raise the temperature of the primary water to 32.2 °C (90 °F) while maintaining a bulk pool water temperature of 37.8 °C (100 °F). Then the temperature of the primary coolant water will be slowly raised to 54.4 °C (130 °F). The position of one control blade or the regulating blade will be adjusted to compensate for any

reactivity changes to keep the reactor critical. Once the primary coolant temperature coefficient has been determined, the pool temperature coefficient will be measured in a similar fashion. In this test, the primary coolant water will be kept at 54.4 °C while the pool water temperature will vary from 32.2 °C to 54.4 °C. It should be noted that during this test, the temperature of the water in the center flux trap and the bulk pool will change. Because the core reactivity change due to pool water temperature changes will be small, it is expected that the position of the regulating blade will be adjusted to compensate for any reactivity changes to keep the reactor critical.

Predictions of the primary and pool coolant temperature coefficients for the fresh LEU core have been completed using MCNP5. For both the primary and pool temperature coefficients, five MCNP5 models were prepared with the water of the coolant system under analysis increasing in 5.5 °F (10 °F) increments, from 32.2 °C to 54.4 °C (90 °F to 130 °F). Due to the low power of this test, the fuel and cladding of the fuel elements were assumed to be isothermal with the primary coolant water. The center flux trap was assumed to be loaded with an empty experiment holder, but there were no experiments modeled in the flux trap or the graphite reflector. As the temperature of the primary coolant or pool water was increased, both the water temperature and corresponding density were changed in the model. The reactivity change due to water temperature change will be primarily from changes to the water density. Figure 15 and Figure 16 show the calculated primary and pool water temperature coefficient of reactivity for the fresh LEU core with the associated 2σ uncertainty of the analysis. For comparison purposes, measured values for the fresh HEU core obtained from [21] are also provided.

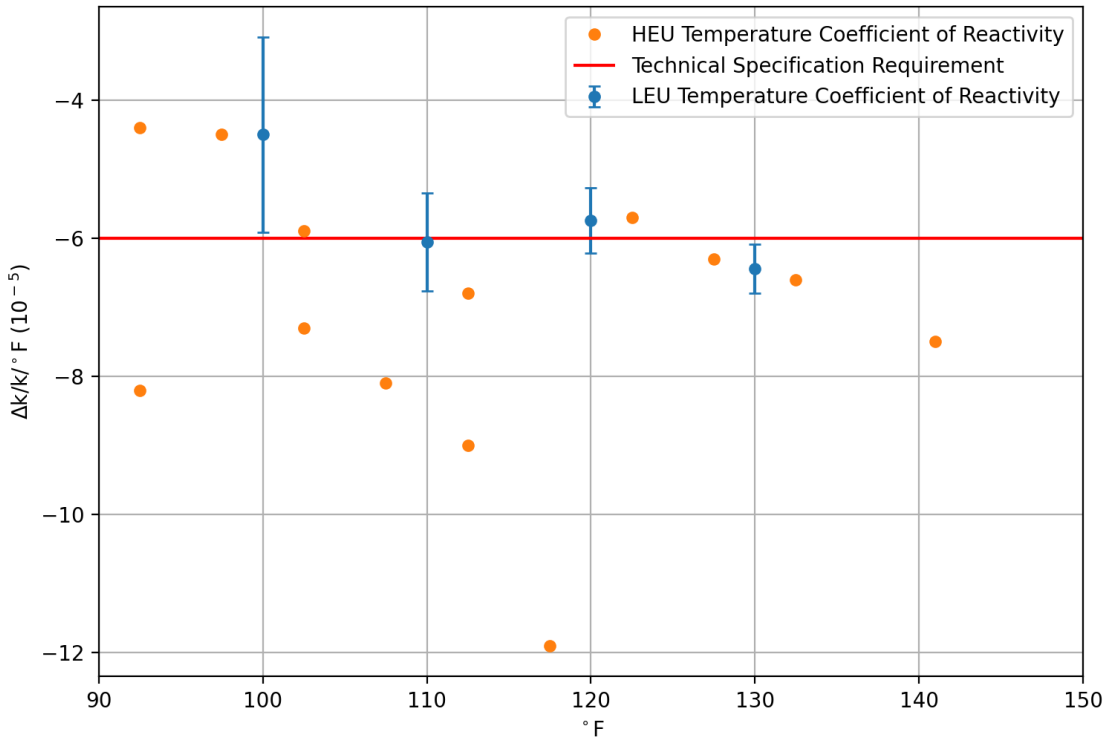

Figure 15: Primary Temperature Coefficient of Reactivity for Fresh LEU Core, Measured HEU Values, and Technical Specification Limit

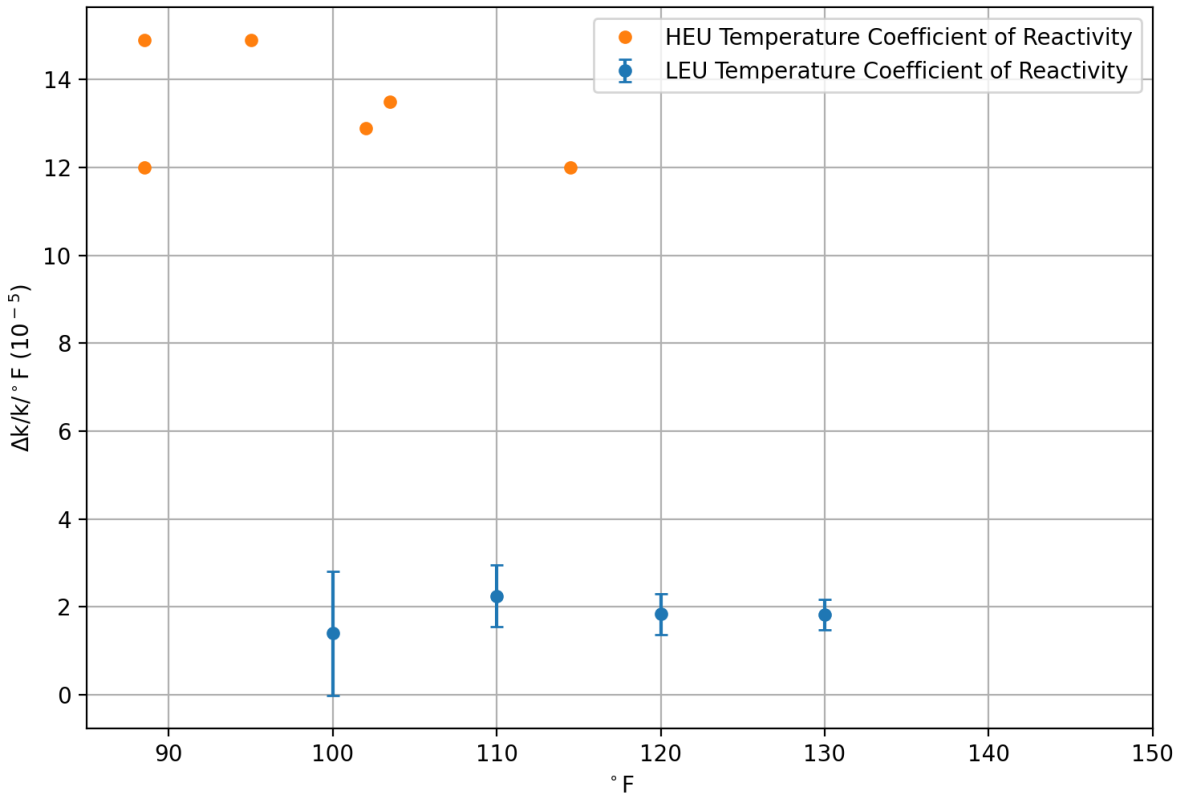

Figure 16: Pool Temperature Coefficient of Reactivity for Fresh LEU Core

As can be observed in Figure 15, the primary coolant temperature coefficient of reactivity results for the fresh LEU core are in reasonable agreement with the measured primary coolant temperature coefficient of reactivity for the HEU fuel. While there is some significant scatter in the measured and predicted results, the magnitude of the primary temperature coefficient appears to generally increase with coolant temperature for both HEU and LEU fuel, with the least negative values occurring when the primary coolant temperature is at the low range of the startup test. This phenomenon was also seen in the MITR LEU model benchmarking analysis and the MITR HEU Safety Analysis Report [22] [29]. MURR's technical specifications require the primary coolant temperature coefficient of reactivity to be more negative than -6×10^{-5} Δk/k/°F. The analysis predicts that this requirement will be met at primary coolant temperatures that are in the range of normal MURR operations at full power for the LEU core (> 48.9 °C). Further, more

detailed analysis at higher temperatures could also be done if the results of the startup test are inconclusive.

The pool temperature coefficient of reactivity has no Technical Specification requirement. The predicted pool temperature coefficient for the fresh LEU core has an average value of $+1.82\times10^{-5}$ Δk/k/°F over the range of temperatures examined (90 to 130 °F). This is much smaller than the measured pool temperature coefficient for the fresh HEU core reported in [21], which had an average measured value of $+13.4\times10^{-5}$ Δk/k/°F over the temperature range from 86 to 116 °F. It is expected that the pool temperature coefficient will differ between HEU and LEU, but it seems unlikely that changes to the fuel element design would result in a decrease in the temperature coefficient by more than a factor of 7 from the use of LEU relative to HEU observed here. This is especially unexpected because the largest contribution to the pool temperature coefficient are reactivity changes resulting from water density changes in the flux trap and, as discussed in Section 3, the flux trap void coefficient of reactivity for the LEU fuel is predicted to be similar to that for the HEU fuel. One possible explanation for the differences which have been observed between the measured and predicted pool temperature coefficient may be the difficulty in establishing the temperature for the bulk pool water during the startup test performed for the HEU core. Because of the large volume of water in the pool (approximately 106,000 liters), it is unlikely that the pool water was at a uniform temperature during the data collection for the HEU core, which is the assumption made in the LEU predictions. Two sets of thermocouples, one near the graphite reflector region and another in the flux trap, were used during the HEU test to determine the bulk pool temperature. A mitigation strategy may be to place more thermocouples in the pool to more accurately determine the pool temperature during the startup tests for the LEU core when they are completed.

8) Measurement of the Neutron Flux Distribution in the Experimental Positions

To accurately characterize the neutron flux distribution with the LEU fuel element design, MURR will measure the flux in several experimental positions throughout the core as the last of the startup tests. There are four positions where the flux may be measured in the reactor as it is currently configured: Tube A of the 6-barrel flux trap experiment holder and the N1, G1, and H1 irradiation positions in the graphite reflector region. These positions are highlighted in Figure 17. The reactor will operate at full power (12 MW) for one hour for this test. Diluted cobalt in aluminum wires will be used for activation analysis in order to measure the neutron flux. ^{59}Co (100% natural abundance) has a thermal neutron capture cross-section of approximately 40 barns and is commonly used for thermal neutron fluence determinations [30].

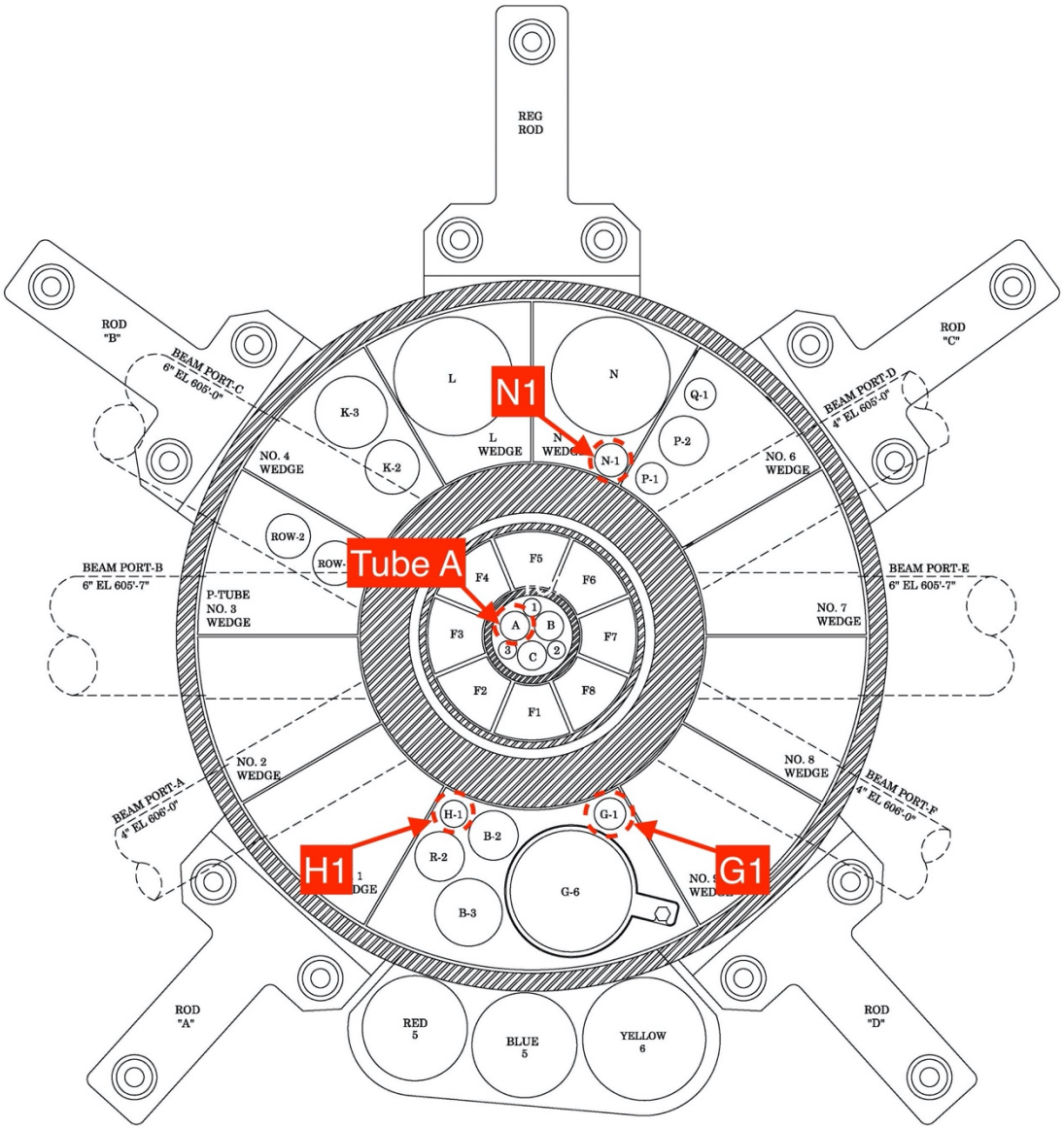

Figure 17: Tube A, G1, H1, and N1 Positions

Measurements will be taken for both xenon-free conditions and when the fuel elements reach equilibrium xenon conditions after approximately 48 hours. While experimental flux results for the all-fresh LEU core will be presented in the transition core analysis, these results will be presented in terms of performance relative to the current HEU fuel with the core operating at 10 MW. To predict the neutron flux for the LEU core, 0.1% Co-Al wires were

modeled in MCNP5 in Tube A of the center flux trap and the G1, H1, and N1 positions in the graphite reflector. F4 tallies were used in the MCNP5 model to predict the flux incident on the wires in 2.54 cm long segments. Figure 18 presents the predicted thermal (E < 1 eV) and total neutron flux as a function of axial position in Tube A for the fresh LEU core operating at 12 MW. Figure 19 presents the axial flux distribution in the G1, H1, and N1 positions in the graphite reflector for the LEU core at 12 MW. Corresponding plots of the axial flux distributions in Tube A and the graphite reflector positions at equilibrium xenon conditions are provided in Figure 20 and Figure 21, respectively.

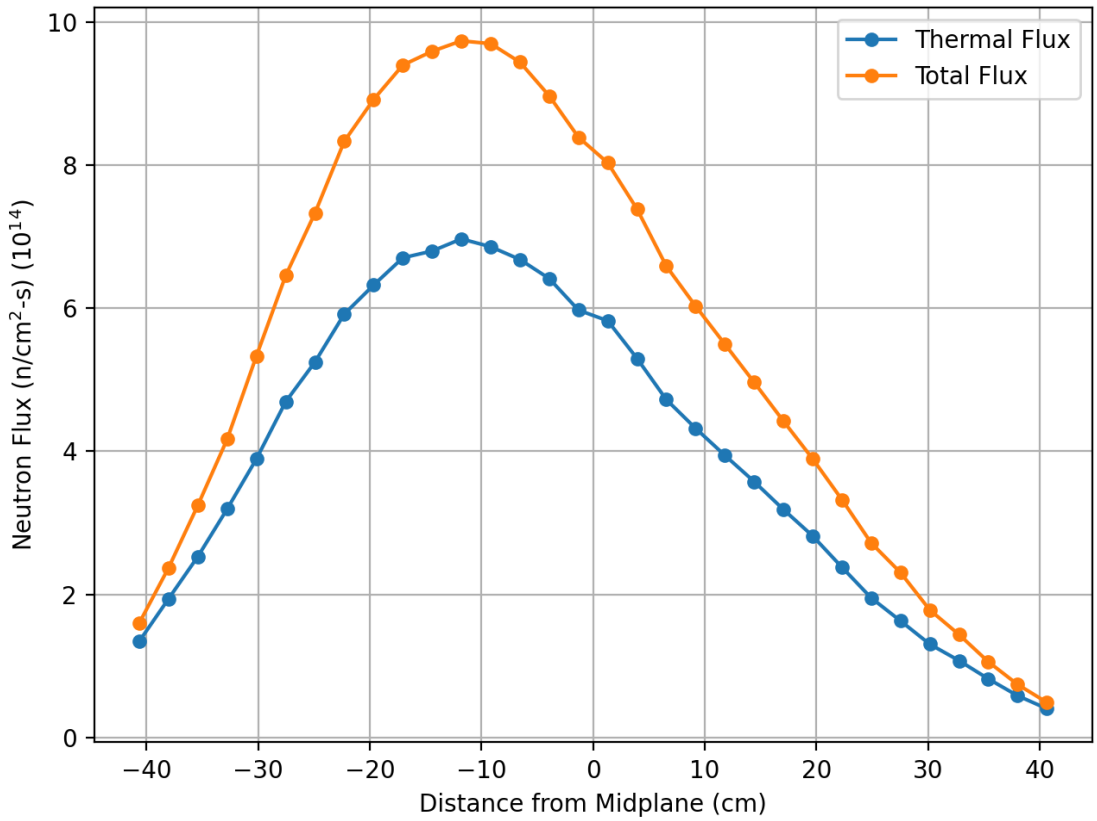

Figure 18: Axial Neutron Flux in Tube A with All-Fresh LEU Core at Xenon-Free Conditions

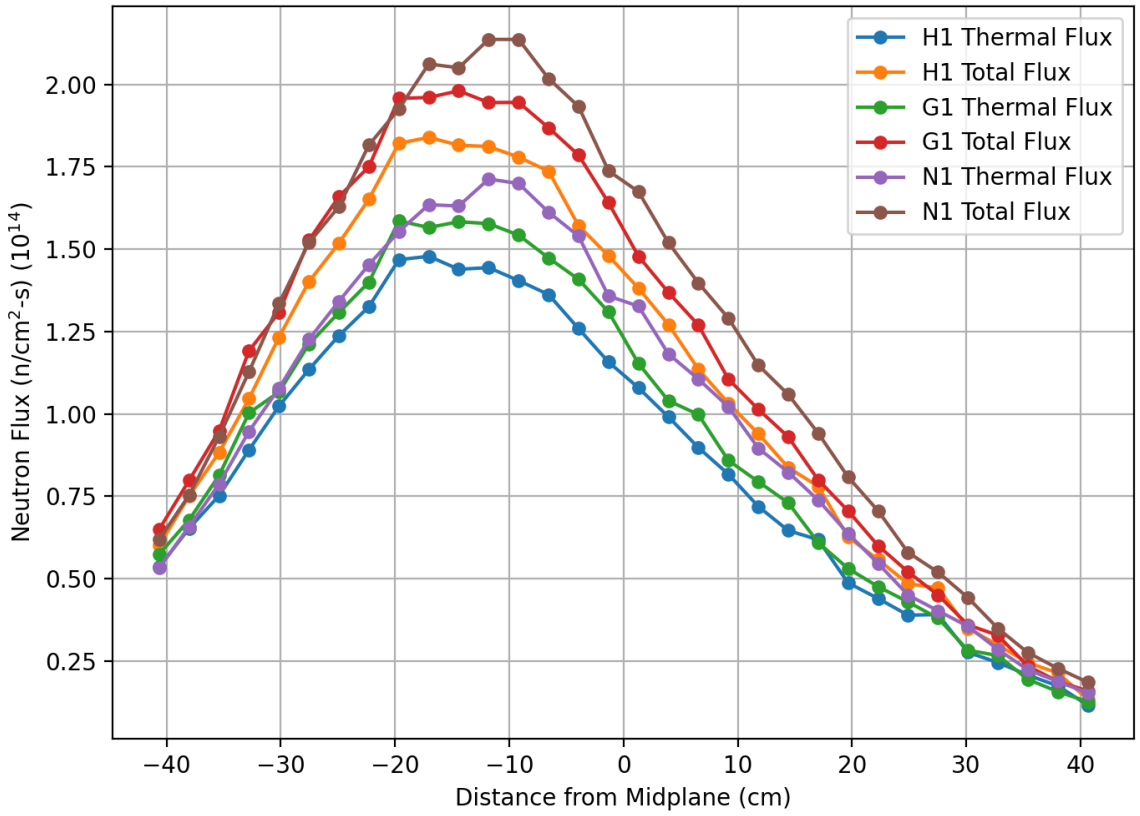

Figure 19: Axial Neutron Flux for G1, H1, and N1 Positions with All-Fresh LEU Core at Xenon-Free Conditions

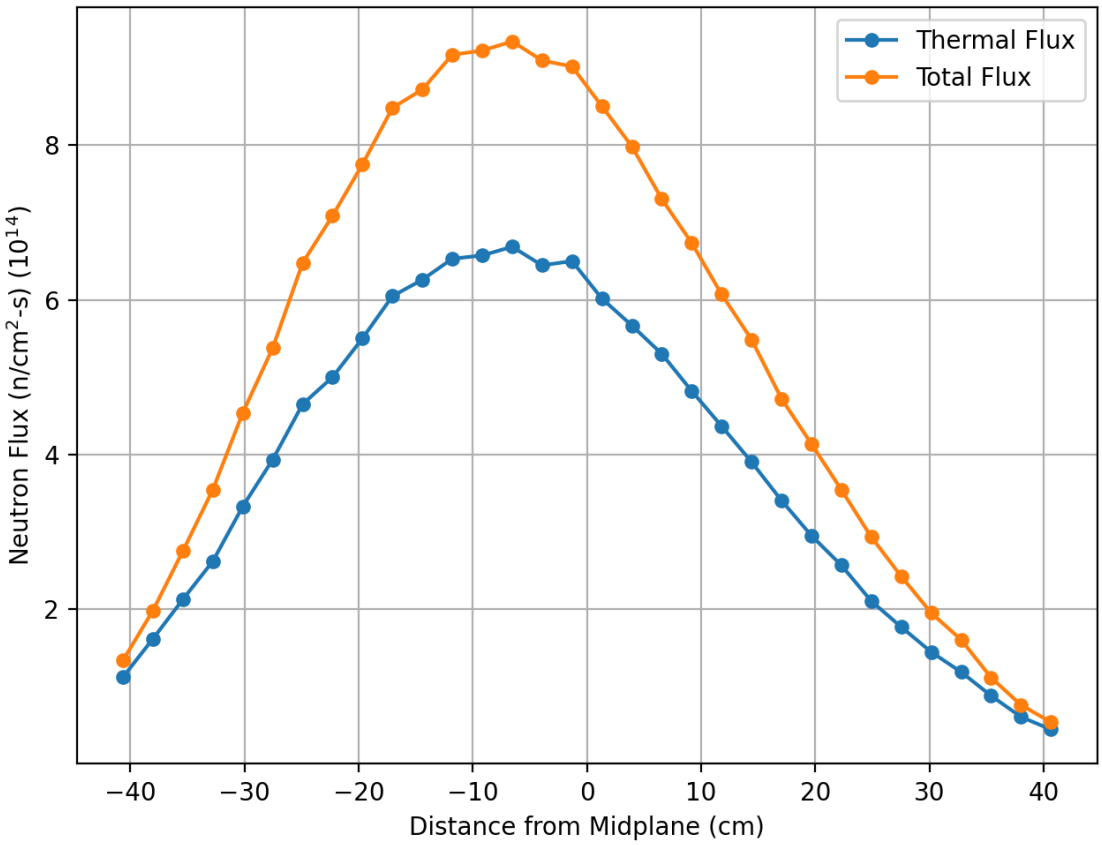

Figure 20: Axial Neutron Flux in Tube A with LEU Core at Equilibrium Xenon Conditions

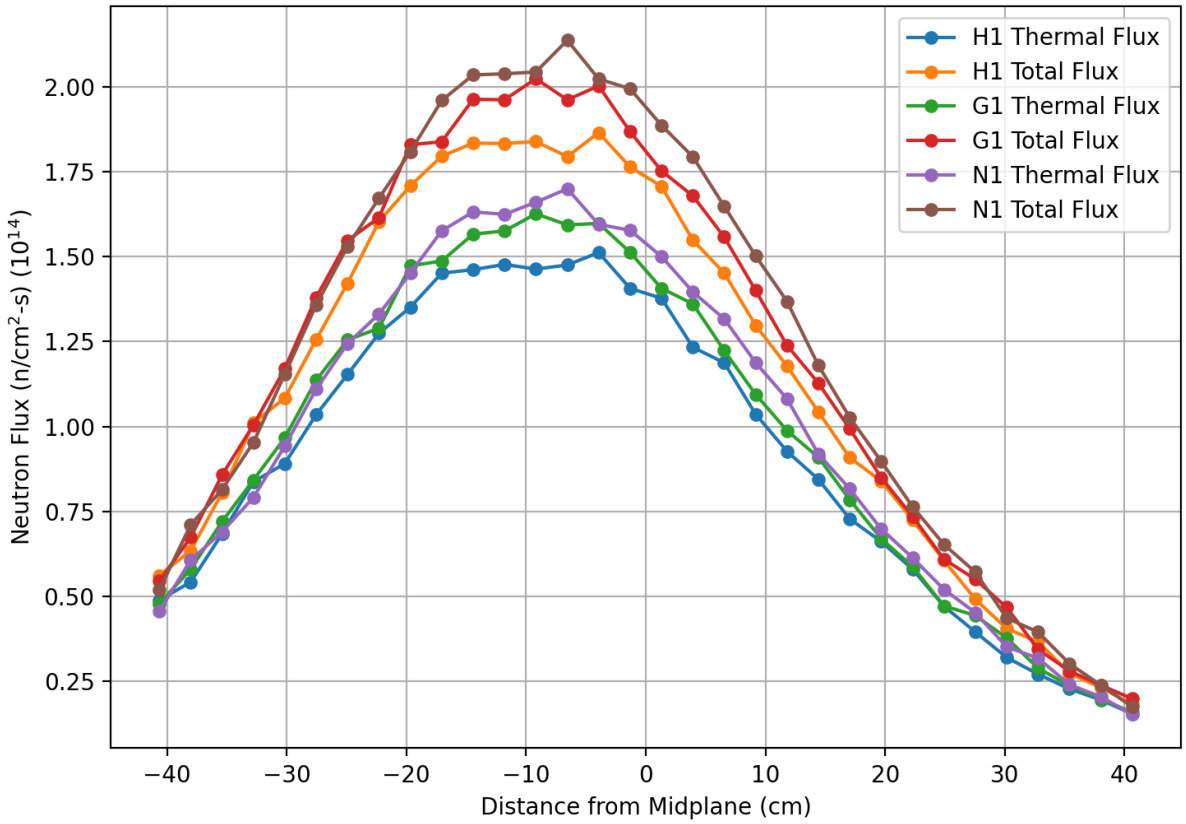

Figure 21: Axial Neutron Flux for G1, H1, and N1 Positions with LEU Core at Equilibrium Xenon Conditions

Figures 18 – 21 illustrate some important aspects of the neutron flux distribution in key experimental positions at MURR. First, it is seen that as xenon builds in during operation, the flux in the experimental positions being monitored becomes slightly more evenly distributed in the axial direction and the location of the maximum flux shifts higher in elevation. Both of these phenomena are due to the withdrawal of the control blades by 10.5 cm in the first 48 hours. Second, there is a slight reduction in the magnitude of the maximum flux in Tube A from xenon-free to equilibrium xenon conditions, while there is a slight increase in the magnitude of the maximum flux in the positions in the graphite reflector during this same time of the operating cycle. This demonstrates how the position of control blades affects the radial power distribution

in the core, shifting the neutron flux distribution from the center flux trap towards the graphite reflector.

Lastly, it should be noted that the predicted critical control blade positions for the initial all-fresh LEU core at xenon-free and equilibrium xenon conditions are 32.03 cm and 41.91 cm, respectively. These critical control blade positions are more deeply inserted than the critical control blade positions which are typically about 43 cm and 58 cm under xenon-free and equilibrium xenon conditions, respectively. As a result, the neutron flux in the experimental positions in the lower axial regions of the reactor is expected to be greater than typical operations immediately following conversion, while the flux in the upper axial regions will be reduced relative to typical operations. Strategies that will largely be dependent on experiment needs at the time of LEU conversion are being devised by MURR operations staff to mitigate any experimental performance loss until the burnup of the available fuel element inventory is sufficient to allow a return to typical operations. This is discussed in the following chapter.

D. CONCLUSIONS

In order to quantify reactor physics parameters and ensure the behavior of the new LEU core is well-understood by the reactor operator, MURR will perform a series of low-power startup physics tests on the all-fresh LEU core when MURR converts from HEU to LEU fuel. A startup test plan is required by the NRC, and guidance is provided to non-power licensees in NUREG-1537. The relevant section of NUREG-1537 for this analysis can be found in Section 12.11, which states the physics parameters the startup test should analyze. In 1971, when MURR

converted to the current 6.2 kg HEU core, a startup plan was drafted following this guidance. That document was the main template for the MURR LEU startup plan.

The MURR LEU startup plan intends to test nine reactor physics parameters: approach to critical, primary coolant void coefficient of reactivity, flux trap void coefficient of reactivity, determination of reactivity worth of flux trap samples, axial and radial thermal neutron flux distribution, calibration of control blade worth pool and primary coolant temperature coefficient of reactivity, and neutron flux mapping in experiment positions. All of these tests, with the exception of the neutron flux mapping in the experiment positions, will be done at low power. Because of the uniqueness and sensitivity of these tests, MURR will draft detailed procedures and operational checklists to guide operators through the startup tests.

To support the implementation of the startup tests, prediction analysis of the various physics parameters was performed and is presented in this chapter. The primary tool for this analysis was the particle transport code MCNP5, with some post-processing of the MCNP5 output files in Python to calculate error propagation statistics. All the results from this prediction analysis are compared to prior measurements with the current HEU fuel and provide a basis of support for the startup tests, as well as confidence that the physics parameters studied in this analysis will not be adversely impacted by the conversion to LEU fuel.

The age of reactor components, particularly the beryllium reflector and the control blades, could have a large impact on the results of the startup tests. Irradiation of these components during normal operations are expected to affect the core excess reactivity, shutdown margin, effectiveness of the control blades, and the neutron flux distribution. For example, due primarily to high-energy neutron reactions in beryllium, various helium and lithium isotopes build up in the reflector over time, which introduce negative reactivity. Additionally, the boron

in the control blades burns out over time due to neutron capture, decreasing their negative reactivity worth, especially in the areas of the blades that experience the greatest neutron flux. In the current analysis, all reactor components were assumed to be fresh. As the time to conversion approaches, confirmatory analysis may need to be completed with the material compositions for these reactor components specific to the core at the time of conversion.

III. TRANSITION CORE ANALYSIS

A. INTRODUCTION

After the startup tests, MURR will begin operation exclusively with LEU fuel. Beginning with the initial insertion of eight fresh (unirradiated) LEU fuel elements at conversion, there will be a series of transition cores until MURR is able to operate with typical mixed-burnup cores that maintain a relatively fixed core burnup from cycle-to-cycle and support MURR's mission to provide stable and predictable services to the scientific and medical communities. Consequently, MURR will operate atypically for some period after converting from HEU to LEU fuel until there are a sufficient number of LEU elements with a mixture of burnup available for use to achieve prototypic operations. The focus of this chapter is the presentation of a methodology that has been developed to identify candidate transition sequences from all fresh LEU cores to MURR's typical operating conditions, with an objective of minimizing the length of the transition period. Each candidate sequence was further evaluated against constraints imposed by the reactor operator, including experimental performance measures and safety margins. A proposed sequence of transition cores that satisfies these constraints is also presented.

During the MURR operating cycle, the positioning of the control blades that is needed to compensate for the core excess reactivity affects the axial and radial neutron flux distribution in experimental locations. With HEU fuel in a typical MURR weekly operating cycle, the control blade position at startup (xenon-free conditions) is approximately 43 cm (out of a full blade travel length of 66 cm), and approximately 58 cm at equilibrium xenon, which occurs after about 48 hours of operation. If the excess reactivity of the fresh LEU fuel requires the control blades to

be more deeply inserted than what is typical, the neutron flux will be compressed towards the bottom of the core. This will reduce the experimental performance in irradiation positions above the core midplane relative to a typical MURR HEU operating cycle.

In previous work, transition cycles were analyzed with a core layout consistent with the MURR LEU Conversion Preliminary Safety Analysis Report (PSAR) [31]. Specialized "transition elements" with a burnable absorber incorporated into the LEU element in the form of borated side plates as a mechanism for reactivity hold-down were considered in order for MURR to operate with control blade positions that are similar to prototypic HEU operation. It was found through analysis that side plate material (AA6061) with the addition of approximately 1300 ppm boron in these transition LEU fuel elements would maintain control blade positions that are typical for HEU operations for an all fresh LEU core. Using a typical MURR fuel management scheme, it was found that along with the fabrication of 12 transition LEU elements (elements with borated side plates) and 24 standard LEU elements (elements with no borated side plates) during the first year of operation following conversion, it would take 49 transition cycles before MURR would operate with an equilibrium core burnup and no transition elements. Given the challenges of a material qualification program for the borated side plate material plus the higher anticipated cost of specialized transition LEU elements with burnable absorbers relative to the cost of standard LEU elements, it has been considered beneficial to explore alternative strategies that would eliminate the need for any special transition fuel elements for MURR. That determination, in conjunction with the need to perform more detailed analyses of safety margins and experimental performance for the transition cores, has motivated the present work which explores the exclusive use of the preliminary LEU fuel element design during the transition sequence.

One of the goals of conversion is to maintain existing operating practices and performance at the facility wherever practical. Consequently, in order to plan the transition cycles, it is necessary to understand the current HEU fuel management scheme so that the LEU fuel management can match the current HEU fuel management where possible. A typical HEU core consists of eight elements with a range of burnups. The target for the total core burnup at BOC is 572 ± 20 MWd. This is a facility-specific practice that maintains appropriate excess reactivity in the core, thus allowing the control blades to be withdrawn to an optimal position when equilibrium xenon is reached and beyond, which provides the ideal flux profile across the core that MURR experimenters require. The ±20 MWd range on the core burnup provides sufficient operational flexibility while also maintaining stable and predictable performance for MURR's irradiation services.

The operating time each week is approximately 6.3 days, with the rest of the week dedicated to maintenance, refueling, and experiment change out. After the reactor is shutdown, all eight elements are taken out of the core. These elements are not available to be used for the next cycle due to the xenon content that is still present in the element at startup of the next cycle. Rather, the core loading is selected from the remaining elements in the active fuel cycle, which typically consists of about 32 elements. Based on prior peaking analysis, elements are discharged from the fuel cycle after achieving a total burnup of 150 MWd [7]. As elements are discharged, new elements are introduced into the reactor in pairs, and are kept paired together throughout their lifetime. MURR typically uses 22 new fuel elements each year to maintain its operations.

Where possible, in order to minimize the differences in operation from HEU to LEU fuel, the transition fuel management scheme attempted to mimic the current HEU fuel management scheme. Specifically, the transition fuel management scheme 1) introduced LEU elements in

pairs, 2) assumed a discharge burnup limit of 180 MWd per element, 3) prohibited the use of elements in back-to-back cycles (except for the first six weeks of the transition sequence, as discussed below), and 4) targeted a total core burnup at BOC of 687 MWd ± 24 MWd. The targeted BOC burnup for the LEU fuel cycle is based on the equilibrium fuel cycle analysis performed in Reference [31], which was found to preserve experimental performance and safety margins at 12 MW operation with LEU relative to 10 MW operation with HEU. The core burnup range of ±24 MWd is selected as a 20% increase from the HEU target core burnup and band. In addition to fuel management, experimental performance and safety margins are the other considerations for the LEU transition cores that must be evaluated. The experimental performance at key locations were identified by the reactor operator. However, rather than mitigating any performance penalty with LEU relative to HEU at particular locations that may occur during the transition sequence, the approach adopted was to arrive at the target equilibrium burnup as quickly as possible during the transition to equilibrium operations to limit the duration of any experimental performance penalties following conversion. Lastly, all cores in the transition sequence were evaluated to ensure that safety margins are satisfied before acceptance of the design.

In the first transition cycle, MURR will operate with eight fresh LEU elements. Because of the excess reactivity of these fresh elements, the control blades must be more deeply inserted than is typical for MURR operations with HEU. In order to assess the magnitude of the experimental performance penalty during the transition cycles relative to current operations with HEU, 454 key experimental locations and flux and reaction rate metrics were identified by experts at MURR. While the MCNP5 model preparation and execution was done at MURR as part of the current work, the postprocessing of the tally results was done at ANL [32]. These

metrics were calculated for the all fresh LEU core in the first transition cycle operating at 12 MW and compared with values calculated for a typical HEU core operating at 10 MW. Even with a 20% uprate in power, this deep insertion of the control blades reduces the experimental performance, particularly in the upper part of the reactor. This is shown in Figure 22, which plots the performance for all metrics for the all fresh LEU core relative to the prototypic HEU core. It was found that for 177 metrics, mostly those above the core midplane, the experimental performance in the all fresh LEU core is lower than that for the HEU core by as much as 33%.

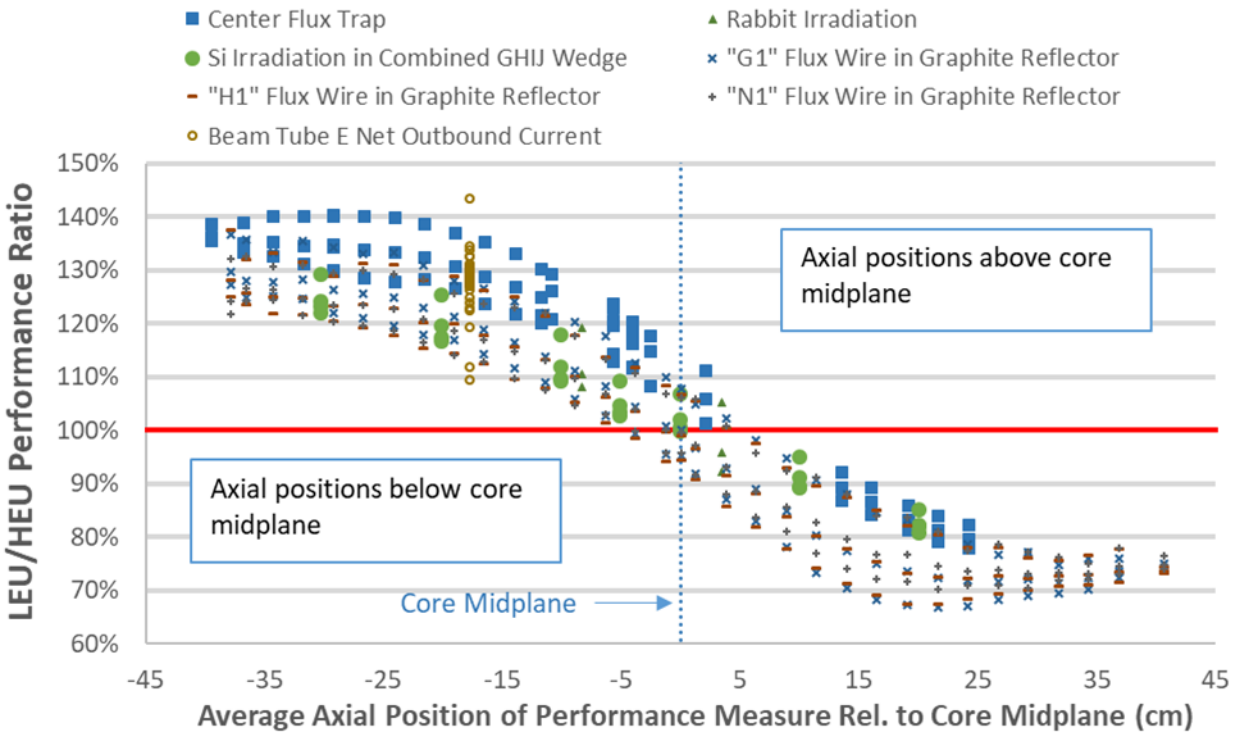

Figure 22: MURR LEU Cycle 1 Total Weekly performance at 12 MW Relative to Prototypic HEU Performance at 10 MW

B. METHODOLOGY

As introduced above, the stated purpose of this work is to identify a sequence of transition cycles following conversion to LEU that will meet MURR's operational and safety criteria. A methodology has been developed to identify candidate transition sequences from all fresh LEU cores to MURR's typical operating conditions, with an objective of minimizing the length of the transition period. Each candidate sequence was evaluated against constraints imposed by the reactor operator, including experimental performance measures and safety margins.

In order to efficiently evaluate candidate transition sequences, a Python program was written which selected the optimal core, given the available fuel elements, for any given cycle, taking into account all of the identified constraints. The program is presented in Appendix A. Rather than using MCNP5 or DIF3D for the initial evaluation of the candidate cycles, this simplified simulation assumed equal power sharing among the eight fuel elements in the core for predicting the element burnup.

Because performance has been identified as a key challenge for the LEU core transition cycles, it is desirable to devise a scheme that quickly moves through the transition cycles to equilibrium operations within the MURR operating constraints described above. The easiest way to do this is to burn elements in back-to-back cycles, which will most rapidly increase the core burnup and result in critical control blade positions that will cause less compression of the neutron flux towards the bottom of the core. While this is not typical or feasible for current operations at MURR with HEU fuel, the LEU elements will initially have relatively low burnup and enough excess reactivity to overcome the xenon poisoning in these elements at startup. Preliminary analysis found that the LEU fuel element design has enough excess reactivity to operate in this fashion for six back-to-back cycles. Consequently, the program assumed the same

eight LEU elements will be loaded for the first six weeks before introducing eight new elements. After week six, elements were not allowed to be used in back-to-back cycles in order to be consistent with current operations.

It is noted, however, that operating in this matter will result in a departure from normal control blade insertion patterns. For a prototypic core with no xenon in the elements at startup, the control blades are positioned at around 43 cm (about 12.5 cm above the core midplane), and are quickly withdrawn over the course of the first 48 hours as xenon builds in. With this new approach, the control blades at startup for weeks two through six will be positioned at a higher axial level than at the equilibrium xenon condition. The impact of this change to typical operations on core power distributions and thermal-hydraulic performance must also be evaluated to ensure that adequate safety margins are maintained.

In order to limit the number of elements needed for the first year to within a target fabrication capacity of 36 elements, the Python program only allowed the introduction of two fresh elements every fifth week for the first year after conversion. After the first year, the program allowed the introduction of two fresh elements whenever needed to meet the fuel management requirements, up to a limit of 32 LEU elements in the active fuel inventory. This is consistent with current MURR operations that typically has 32 HEU elements in the active fuel inventory. For each cycle, the Python program searched all possible combinations of previously irradiated and fresh elements, while observing the specified constraints, to find a set of eight elements that was closest to having a BOC core burnup of 687 MWd. It should be noted that, in order to ensure that there was sufficient excess reactivity for the 6.3-day cycle, the core burnup of all transition cycles could not exceed 711 MWd (687 + 24). However, it was allowed to drop

below 663 MWd (687 – 24) if no suitable collection of eight elements could be found that was within the band.

C. RESULTS

Given the constraints of MURR safety margins, operations, production and research, and to limit the number of fuel elements required in a time period after conversion to LEU fuel, multiple transition sequences were evaluated. A sequence of transition cycles that meet the imposed constraints for fuel management and safety margins is presented in Figure 23. This figure provides an overview of the transition cycles and subsequent prototypic LEU operating cycles over the two years following conversion. The figure shows the BOC core burnup for each cycle estimated by the Python program and the number of elements in the fuel cycle. The figure also identifies cycles in which fresh LEU elements are loaded into the core. The sequence requires the fabrication of 34 fresh LEU elements during the first year following conversion and 30 fresh LEU elements in year two. Though not shown in Figure 23, the Python program calculated that 22 fresh LEU elements will be needed in year three, which is typical for current operations with HEU. It is also important to note that this transition sequence, with the requirement of 34 fresh LEU elements during the first year, represents an improvement over the previous transition cycle approach presented in Reference [31], which required the fabrication of 36 fresh fuel elements in the first year, 12 of which were specialized elements with burnable absorbers. The approach developed here requires only 34 fresh LEU elements in the first year and no specialized elements with burnable absorbers.

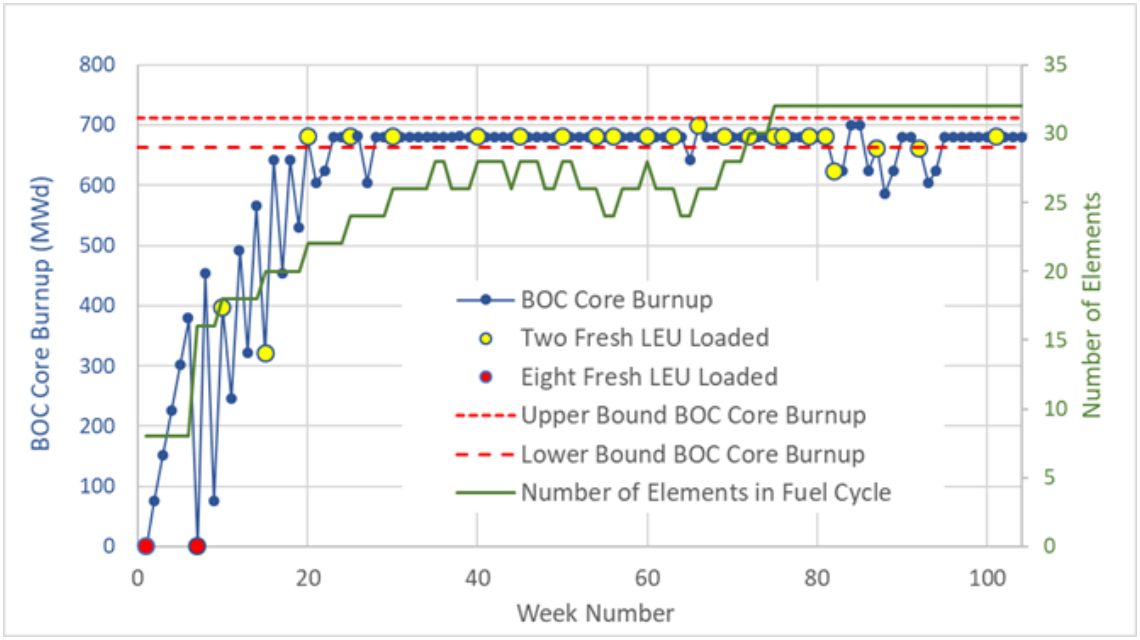

Figure 23: Beginning-of-Cycle Core Burnup and Number of Elements in Inventory during Approach to the LEU MURR Equilibrium Burnup Cores

Although this chapter is not focused on presenting the details of experimental performance or how MURR will accommodate changes to the performance during the transition cycles, it has been found that the performance penalties (due to the neutron flux asymmetry describe previously) generally decrease over the first 20 weeks of the proposed transition sequence. After week 30, the operating cycle is considered to be in equilibrium, with a LEU core burnup at BOC that is quite stable and within the ±24 MWd band around 687 MWd (i.e., within 3.5% of the target burnup), with the exception of a few anomalous cycles around week 65 and from weeks 82 to 95. Furthermore, this transition sequence does not rely on using a number of fresh LEU fuel elements that would be outside the capability of the fuel manufacturer. By week 75, MURR will have 32 elements in the active fuel inventory, which is typical for current operations and affords flexibility in the planning of weekly core loadings and the availability of "backup" cores that are occasionally needed due to unanticipated mid-week cycle shutdowns and startups.

The sequence of transition cycles summarized in Figure 23 was modeled from weeks 1 to 49 with REBUS-DIF3D to obtain depleted fuel compositions by plate and axial level for all elements in each cycle. These compositions where then used to prepare detailed MCNP5 models for selected cores that were considered of greatest interest. The critical control blade heights were determined for each of these cores and detailed three-dimensional flux and power distributions were calculated to be used for experimental performance and safety analyses.

A critical assumption in the Python program used to initially identify the transition sequence is that, no matter the element burnup, each element contributes an equal share of the total core power. In other words, of the 12 MW of the total core power, each element in the core is assumed to contribute 1.5 MW (one-eighth of 12 MW). This was a crucial assumption that provided a way to efficiently develop candidate transition sequences without the computational expense of a neutronics analysis.

After the burnup of the fuel elements in the transition cycles were calculated with REBUS-DIF3D, the accuracy of this assumption was evaluated by comparing the calculated element burnup at BOC from the neutronics analysis with that obtained from the equal power sharing assumption. While the Python program and element loading and cycle information for the REBUS-DIF3D input were written and executed at MURR as part of this work, the evaluation of this assumption was performed at ANL [32]. Figure 24 summarizes this difference in element burnup for each element utilized during the first 49 weeks of LEU operation (identified as MO-001 to MO-032). Results are presented for each cycle in which the LEU element is loaded into the reactor and show that the difference between the calculated element burnup and the burnup based on the assumption of equal power sharing is < 4% (small exceptions are noted for elements MO-021 and MO-029). It is further observed that for the

earliest transition cycles which are loaded with elements that all have similar burnup, the difference between the estimated and actual burnup is smaller in magnitude and varies from +3% to -1%. The difference decreases as the elements are used over multiple cycles and is no more than 1.7% for an element that has reached its discharge burnup of 180 MWd, which is the burnup limit for a MURR LEU fuel element. This brief analysis verifies that the assumption of equal power sharing among the elements in the MURR core is quite reasonable for planning purposes.

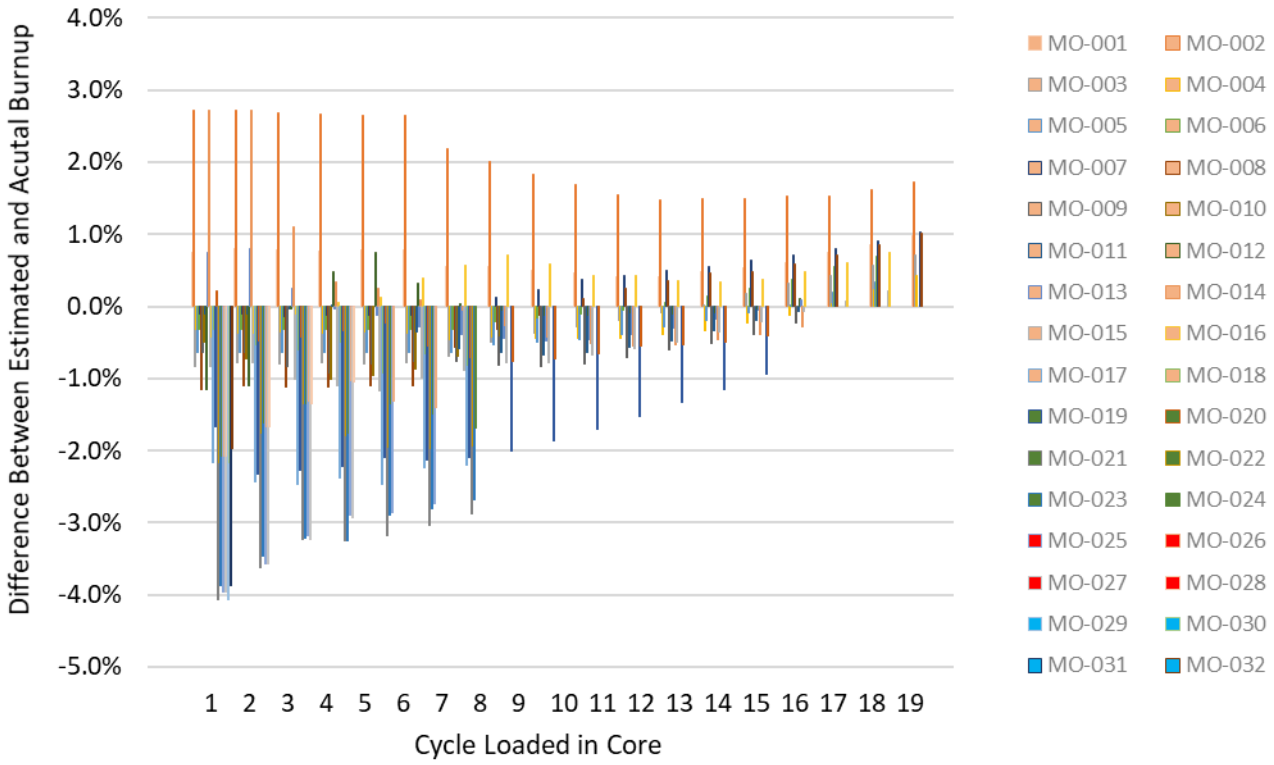

Figure 24: Difference between Estimated and Actual BOC Burnup of Transition Elements Used During First 49 Weeks of Operations

For further evaluation of the transition sequence, it is worthwhile to consider the critical control blade positions during the transition cycles because of their anticipated impact on experimental performance and safety. For estimation purposes, it was assumed that the four BORAL control blades and the beryllium reflector surrounding the core are fresh. Figure 25 shows the predicted critical blade positions during several transition cycles and for the

equilibrium LEU core. Predictions at BOC, equilibrium xenon conditions (two days into the weekly cycle), and EOC (6.3 days) were made with the detailed MCNP5 models. As expected, the critical control blade positions during the cycle are affected by both the core burnup and xenon-state of the core. It is observed, for example, that since increasing the burnup of the core decreases the excess reactivity under xenon-free conditions, and the control blades are at a higher position at startup for cores with greater burnup. Also, as xenon builds in and fuel burnup continues, the control blades are withdrawn even further to maintain criticality.

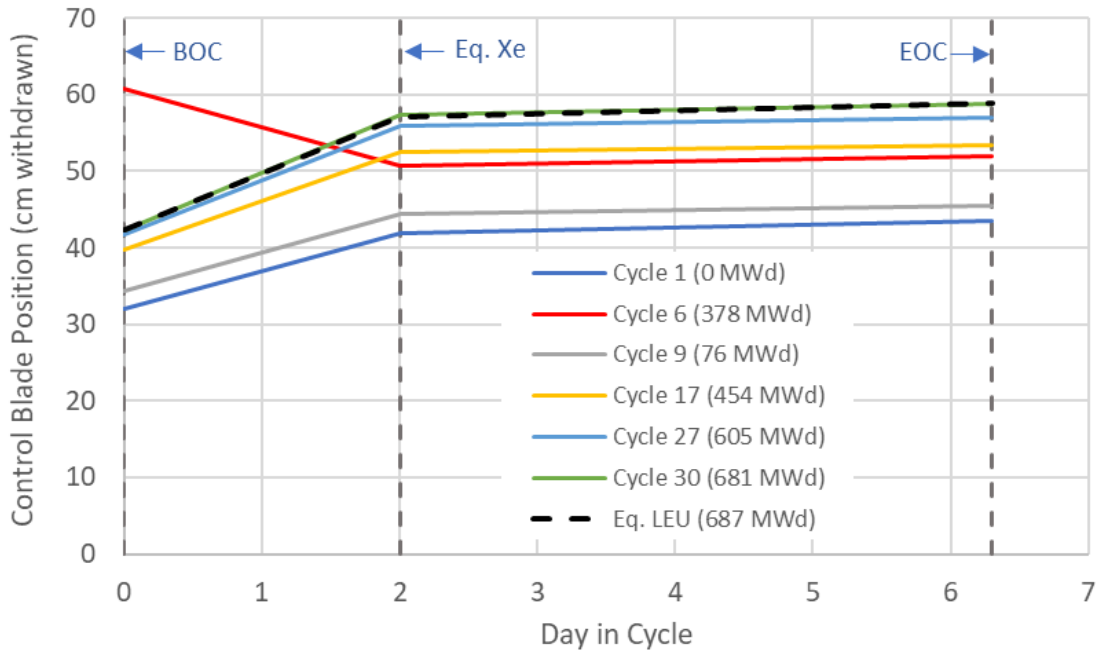

Figure 25: Critical Control Blade Positions during Transition Cycles

It can be seen that for most of the cores evaluated during the first 20 weeks, the control blades at startup and throughout the cycle are less withdrawn (more deeply inserted) than is typical for MURR operations, which is represented by the control blade positions for the equilibrium LEU core. These blade positions suppress the neutron flux in the upper part of the reactor relative to typical operations, while increasing the flux in the lower part. As has been previously discussed, this is obviously not ideal for experiments in the upper part of the reactor.

Furthermore, the change in the control blade positions at a given state point from week-to-week is not preferred for experiments in all parts of the reactor because the weekly variation in the experimental performance in a given position makes it challenging to provide consistent flux levels. This makes it difficult for researchers to predict their experimental performance in advance. However, after week 20, the critical blade positions at startup and throughout the cycle are more in line with the current HEU operations and what has been predicted for equilibrium LEU operations. At week 30, for example, the control blade positions at BOC, eq. Xe, and EOC are within 0.2 cm of those for the equilibrium LEU core under the same assumptions of control blade and beryllium reflector burnup.

Figure 25 illustrates another complication that must be briefly accommodated by MURR operations during the transition cycles. It is planned to use elements in consecutive cycles from weeks one through six. Following the brief shutdown interval between these cycles, substantial xenon poisoning will exist in the elements at BOC. Consequently, as can be seen in Figure 8 for week six, the control blades are positioned about 18 cm higher than is typical at BOC and then are gradually inserted as the core reaches equilibrium xenon conditions. After week six, elements are not used in consecutive weeks, so all elements at BOC are xenon free, which is typical for normal operations for MURR. This can be seen, for example, in the predictions for cycles 9 and following in Figure 25. For most cycles after week 20, and virtually all cycles after week 30, the core burnup is within the target burnup range for equilibrium fuel management. The critical control blade heights for these cycles and beyond follow the typical patterns for MURR operations.

As stated above, 454 key experimental locations and flux and reaction rate metrics were identified by experts at MURR to evaluate the performance of the proposed transition and

equilibrium LEU cores relative to HEU. The MCNP5 output files were postprocessed at ANL to arrive at the final calculated values for the metrics [32]. These metrics were calculated for the LEU cores operating at 12 MW and compared with values calculated for a typical HEU core operating at 10 MW. Figure 26 shows a summary of the calculated performance penalties for these 454 metrics for selected transition cycles over the first 23 weeks. It can be seen that there are performance penalties of 20% or more relative to current HEU operations in some locations during the first 15 weeks of the transition sequence. However, in week 23 of the transition sequence, there is no penalty on performance relative to the current HEU operations for all 454 metrics. Figure 27 further shows that for week 23, the predicted performance at all locations with LEU operations at 12 MW is generally 0% to 10% greater than for HEU operations at 10 MW. The relative performance predictions for all metrics are similar to those predicted for the equilibirum LEU core.

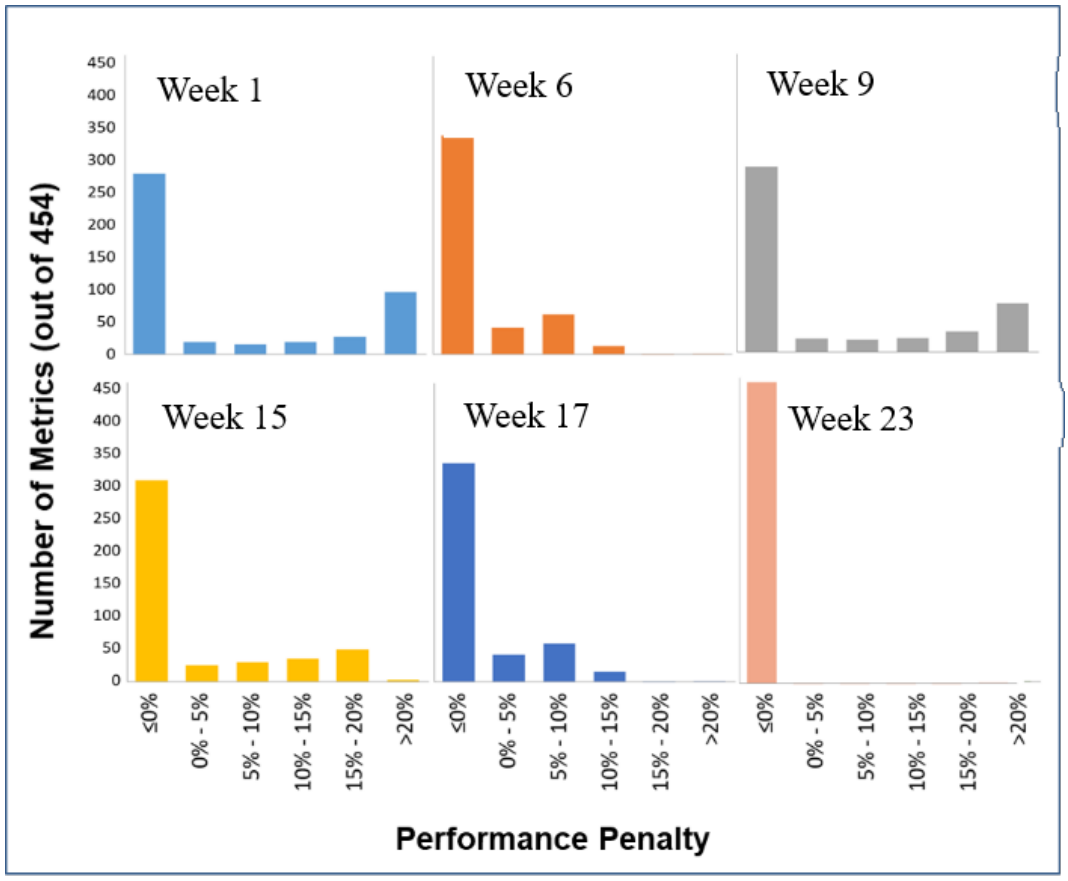

Figure 26: Experimental Performance Penalty for Selected Transition Cycles

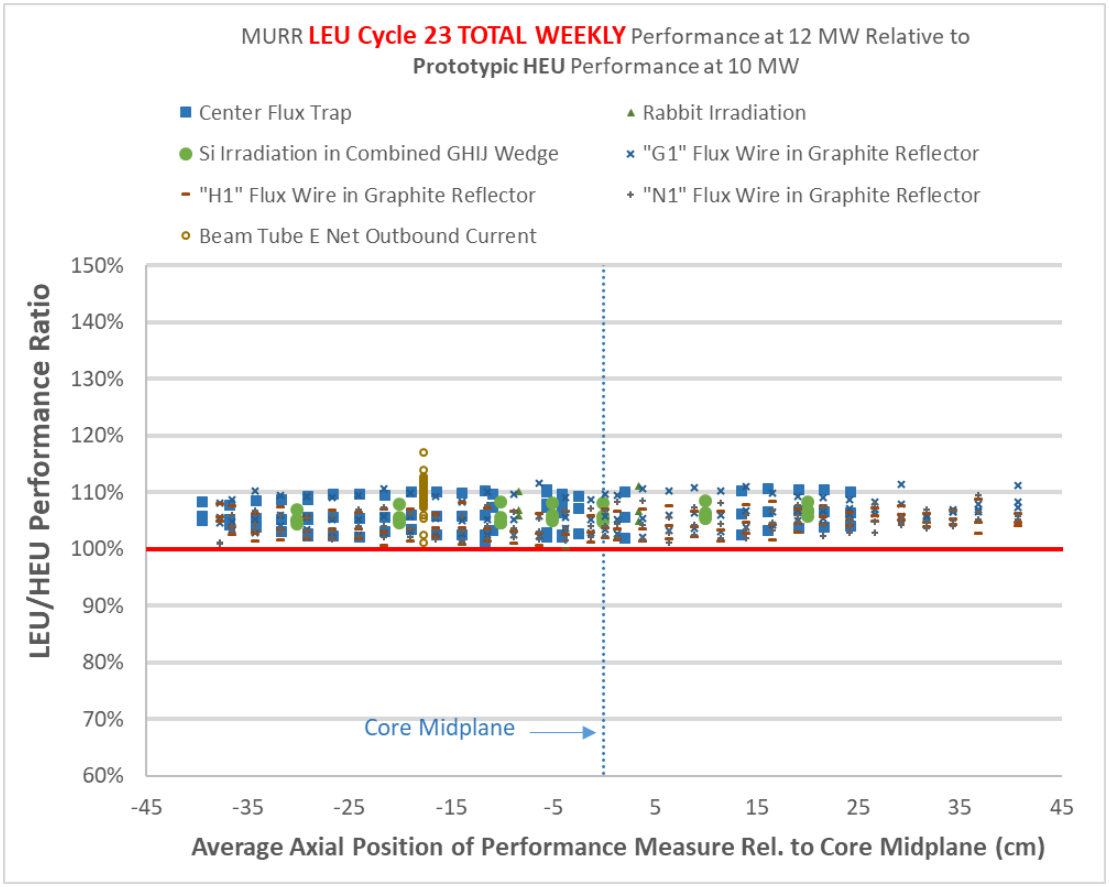

Figure 27: Key Experimental Performance Metrics for Week 23 with LEU at 12 MW Relative to Typical HEU Cycle at 10 MW

Finally, while the safety analysis of the transition cycles is much broader in scope than what could be fully described in this chapter, it is worth some discussion as to whether the transition cycles stay within the required safety margins of MURR. One of the key operational requirements for MURR is that there is adequate margin to the onset of flow instability (OFI) under steady-state operating conditions. The OFI power level is the power at which voiding begins in the coolant channels, which can cause the coolant flow to become unstable. The power level at which this occurs must be greater than the limiting safety system settings (LSSS) power level in order to ensure margin to OFI during all operational conditions, and ideally the OFI power level of all transition cores would be greater than the minimum OFI power level for the

most limiting equilibrium LEU core. Figure 28 shows the OFI power level for selected transition cores. As the graph shows, the minimum OFI power level for the transition cores is 17.49 MW, which is greater than the LSSS power level and similar to the minimum steady-state OFI power level for the equilibrium LEU core.

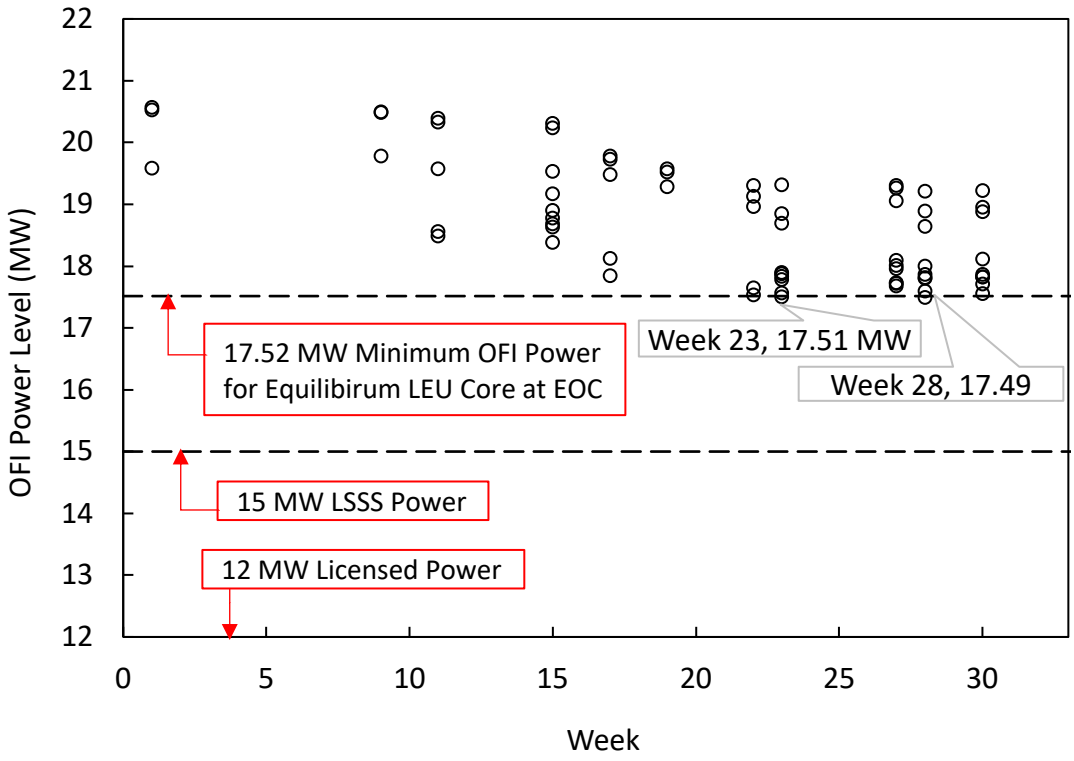

Figure 28: Onset of Flow Instability Power Level for MURR LEU Transition and Equilibrium Cores

D. CONCLUSIONS

The purpose of this work was to develop a methodology for identifying sequences of transition cycles that will enable MURR to transition from all fresh fuel to typical mixed-burnup cores following conversion while meeting operational requirements on experimental performance and safety. Given the constraints of MURR safety margins, operation, production and research, and the USHPRR conversion project, a transition sequence has been proposed that

minimizes the time MURR operates atypically compared to the current prototypic cycles currently using HEU fuel, and moves quickly to the same sort of equilibrium cycles for the LEU fuel that have already been evaluated in documented safety analyses [7]. A LEU cycle is reached that meets or exceeds the level of experimental performance predicted of the prototypic HEU core, but has slightly reduced performance compared to the equilibrium LEU core, in more than 450 key locations by the 23rd week following conversion. Following this, the results show that the BOC core burnup for future idealized cycles is within a narrow band of a target burnup based on the equilibrium LEU core for all but a few cycles and that MURR will consistently be able to meet its performance requirements. This transition sequence also only requires the fabrication of 34 fresh LEU elements in the first year of operation, which is an improvement over the prior work and does not exceed the anticipated availability of fresh elements that can be produced by the fuel fabricator. Combining the short time period before equilibrium burnup is achieved, the small increase of fuel elements needed annually relative to typical operations, and the ability to stay close to the ideal BOC burnup target makes this transition sequence suitable for use when MURR converts to LEU fuel.

Lastly, this chapter has presented only a brief set of results for the critical blade positions during a sequence of transition cycles and an explanation of the effect that these critical positions will have on experiments. A more detailed analysis is necessary to both inform investigators of the performance penalties they may experience during the first 20 weeks in those experimental positions above the core midplane following conversion and the operations team at MURR to mitigate this penalty whenever possible. It may be possible to leverage the increased performance in the lower section of the reactor by repositioning certain experiments to compensate for the lower flux in the upper section, or experiments could remain in the reactor

longer in order to achieve the neutron fluence they require before discharge. Of course, the experiments modeled in the MCNP5 analysis may not be the experiments in the reactor when MURR converts to LEU fuel, so this analysis may be ongoing, depending on the reactor loading and configuration at the time of conversion. Nonetheless, the results presented here, including the experimental performance, core burnup, and critical control blade positions throughout the weekly cycle show that the analyzed transition core fuel management patterns are consistent with what is expected and desired for MURR operation with LEU U-10Mo fuel.

IV. MOLYBDENUM-99 UPGRADE ANALYSIS

A. INTRODUCTION

At MURR, there are three core pillars that shape the mission of the reactor: research, education, and production. Particularly for production, MURR has a long history of providing radioisotopes for pharmaceutical and diagnostic use. TheraSphere™, a therapeutic, has been mentioned in Chapter II. In addition to TheraSphere, MURR currently produces two other FDA-approved drugs: QUADRAMET® and LUTATHERA®. QUADRAMET [33] utilizes the β^- decay of ^{153}Sm to help alleviate pain from bone cancer. LUTATHERA [34] helps treat neuroendocrine tumors with the β^- decay of ^{177}Lu. MURR is also the sole provider of ^{131}I and ^{99}Mo in North America. In total, MURR provides 12 different isotopes to four different countries as a part of their production irradiations.

In 2017, MURR, General Atomics (GA), and Nordion, with a co-operative agreement between GA and NNSA, entered into an agreement to produce fission-based ^{99}Mo at MURR. Currently, MURR produces ^{99}Mo by means of the (n,γ) reaction with ^{98}Mo. This proposed ^{99}Mo production device (referred to as 2017-RBM-99) represented a significant change to the reactor because of the additional heating associated with producing ^{99}Mo by means of fission. The 2017-RBM-99 device was designed to replace two of the graphite reflector elements in the reactor and generate approximately 500 kW of fission power. Such a significant change to the reactor necessitated a safety analysis evaluating the margins to safety previously established both for the current HEU core and the planned LEU core.

Prior to the completion of the project, GA and Nordion withdrew from the partnership for commercial reasons. However, this analysis would still be informative should the project be revived or another fission-based ^{99}Mo source be instituted at MURR. This chapter will focus on

the preliminary analysis of the 2017-RBM-99 device neutronics effects on the LEU core, but the completed analysis, done primarily at ANL, shows that the 2017-RBM-99 device maintains sufficient margins to the established safety parameters for both the current HEU and future LEU cores. [18].

B. RESULTS

In order to accurately calculate the margins to safety, an update of the MURR MCNP model was undertaken. The model that was used before the 2017-RBM-99 upgrade was the MCNP5 model for the preliminary Safety Analysis Report (PSAR), which reflected the reactor configuration as of 2008. There were three main changes to the reactor that had not been incorporated into the 2008 MCNP5 model: use of the six-barrel center flux trap (CFT) experiment holder, implementation of the Flux-trap Irradiations Reactivity Safety Trip (FIRST) device and the combined GHIJ 60° graphite reflector element. The changes can be seen in Figure 29. The FIRST device is an engineered safety system that allows the use of the six-barrel experiment holder in the CFT. The modified experiment holder incorporated three new small barrels, which allows experiments to be removed during reactor operation, in addition to the three large barrels that were previously in the CFT. The 60° combined GHIJ graphite reflector element is primarily used for silicon irradiation.

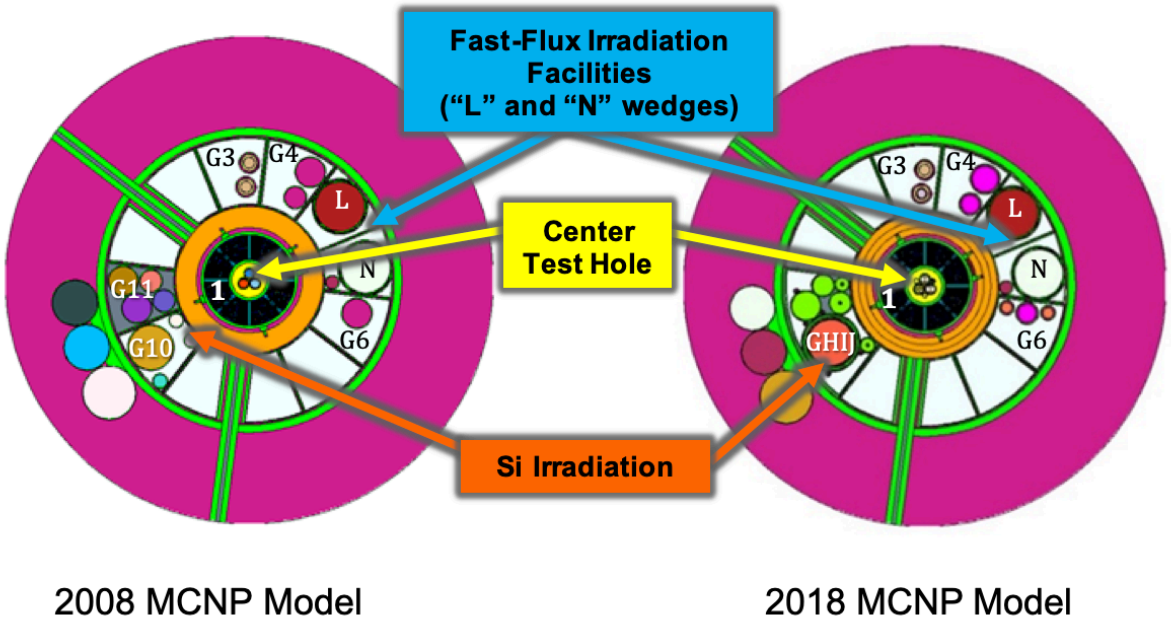

Figure 29: Comparison between 2008 and 2018 MCNP Models

Naturally, any changes to reflector positions or the CFT could result in a significant change in reactivity. As discussed in Chapter II, any change in the CFT affects the neutron balance of the reactor. In order to quantify the reactivity changes, the 2008 MCNP model was updated to the 2018 reactor conditions, and eigenvalue calculations were run. The resulting change was a 0.62% Δk/k reactivity increase from the 2008 model. The excess reactivity for a typical mixed-burnup core with LEU core is 3.6% [8], so these changes represent a non-trivial increase of reactivity.

In order to understand the effects of the 2018 MURR reactor configuration on the power distribution in the LEU design, heat flux calculations were completed to identify the differences between the 2008 and 2018 reactor configurations. Because the CFT experiment holder and its experiments insert a large amount of positive reactivity, this change was studied in detail. The reactivity increase due to the experiment changes caused a change in the critical control blade

positions relative to the 2008 MURR MCNP PSAR model. A Python script was written to efficiently alter and execute MCNP models to predict where the critical control blades heights are for the new reactor configuration. Once the critical blade heights were found, tallies in the MCNP models were used to facilitate comparisons of the axially-averaged hot stripe heat fluxes for the 23 LEU fuel plates in all eight elements. Figure 30 plots the changes to the heat flux profiles for each element in the core between the models. The largest percent change to the heat flux profiles occurs in Plate 1 (plate closest to the flux trap) and is approximately 4%. Figure 30 also shows that the power balance is shifted in the element towards the inner plates and away from the outer plates. For the LEU fuel element design, this has a potentially beneficial impact on the core safety margins. The LEU element is most limited by the OFI in channel 23, so a shift in power away from the outer plates results in an increased margin to safety for the LEU elements. The power shape on plate 1 of the LEU element was also analyzed and is shown in Figure 31. The power shape across the plate is informative in understanding where the power peaking occurs on the plate. Because of the lack of self-shielding near the intersection of the side plates and the fuel plate, the power peaks in these regions. Generally, the azimuthal hot stripe will occur near in this region.

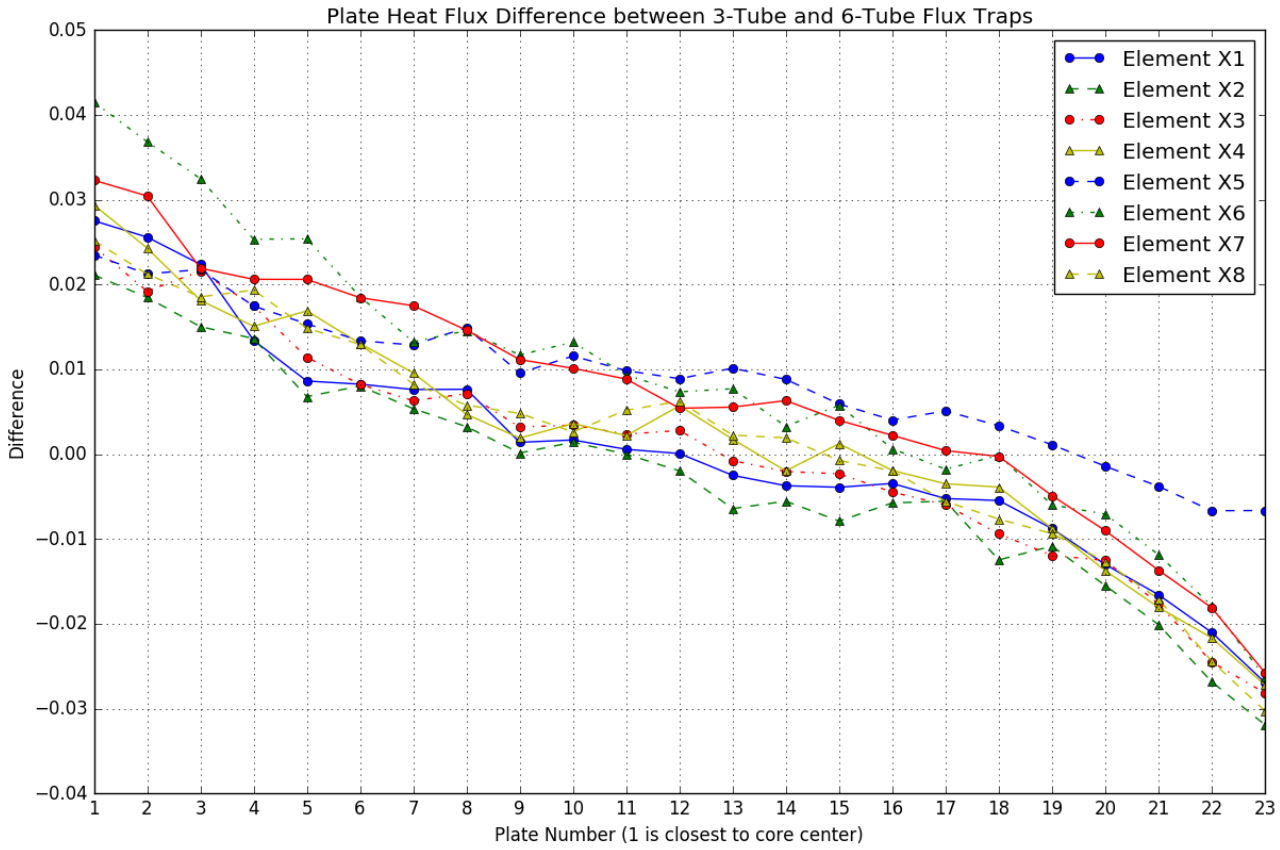

Figure 30: Plate Heat Flux Difference between 3-Tube and 6-Tube Flux Trap

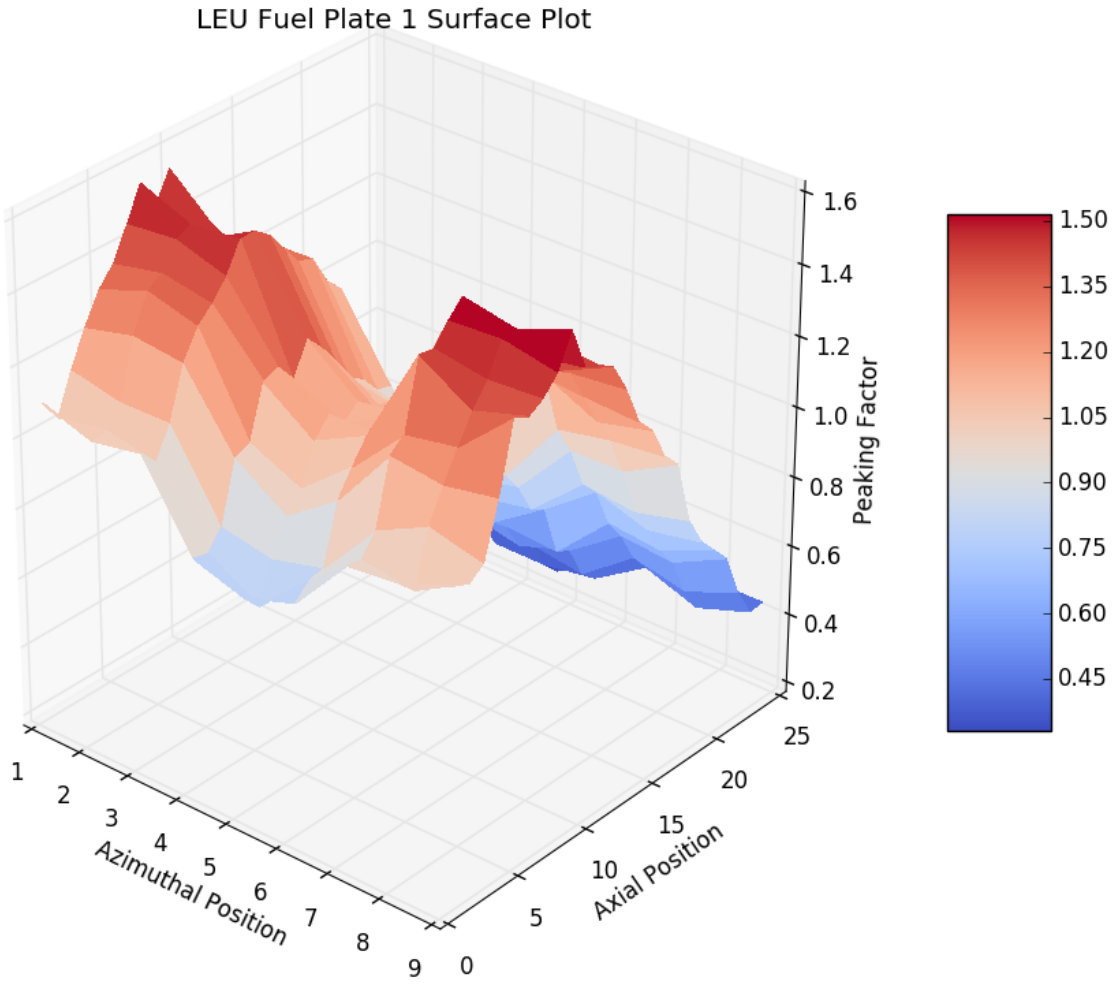

Figure 31: LEU Fuel Plate 1 Surface Plot

After the current changes were analyzed, the 2017-RBM-99 device was inserted in place of the "L" and "N" wedges, and the reactivity was again calculated. The 2017-RBM-99 device added an additional 0.6% Δk/k reactivity for a total reactivity increase of 1.1% Δk/k from the 2008 MCNP MURR PSAR model. With this increase in reactivity and the additional fission heating from the 2017-RBM-99 device, which is located adjacent to the core, there was concern that the preliminary LEU fuel element design may not provide adequate margin to safety, and a redesign of the element may be necessary. In order to provide some initial insight into the effects of the 2017-RBM-99 device on the power distribution of the elements, calculations were done to

compare the axially-averaged heat flux differences between the 2008 MCNP MURR PSAR model and the MURR model with 2017-RBM-99 installed. Of particular interest was the LEU element in core position X5. This element is the closest element to 2017-RBM-99, and it is typically a fresh element. As one of the two fresh elements in the core, the power peaking tends to be higher as these elements have more fissile material than the other six elements. 2017-RBM-99 could also exacerbate this peaking by shifting the power towards the X5 position. Should the heat flux be much greater with the 2017-RBM-99 device, a redesign may be necessary.

As Figure 32 shows, the heat flux in the plates in the X5 position are slightly higher than the heat fluxes calculated with the 2008 MURR MCNP PSAR model. Although the peak heat fluxes differed by less than 10 W/cm^2, the increase of the heat flux in the outer plates of the LEU fuel element relative to the heat flux for the same plates in the LEU element that was calculated during the analysis for the PSAR indicated that further thermal-hydraulics and accident analyses was necessary to determine the margins to safety.

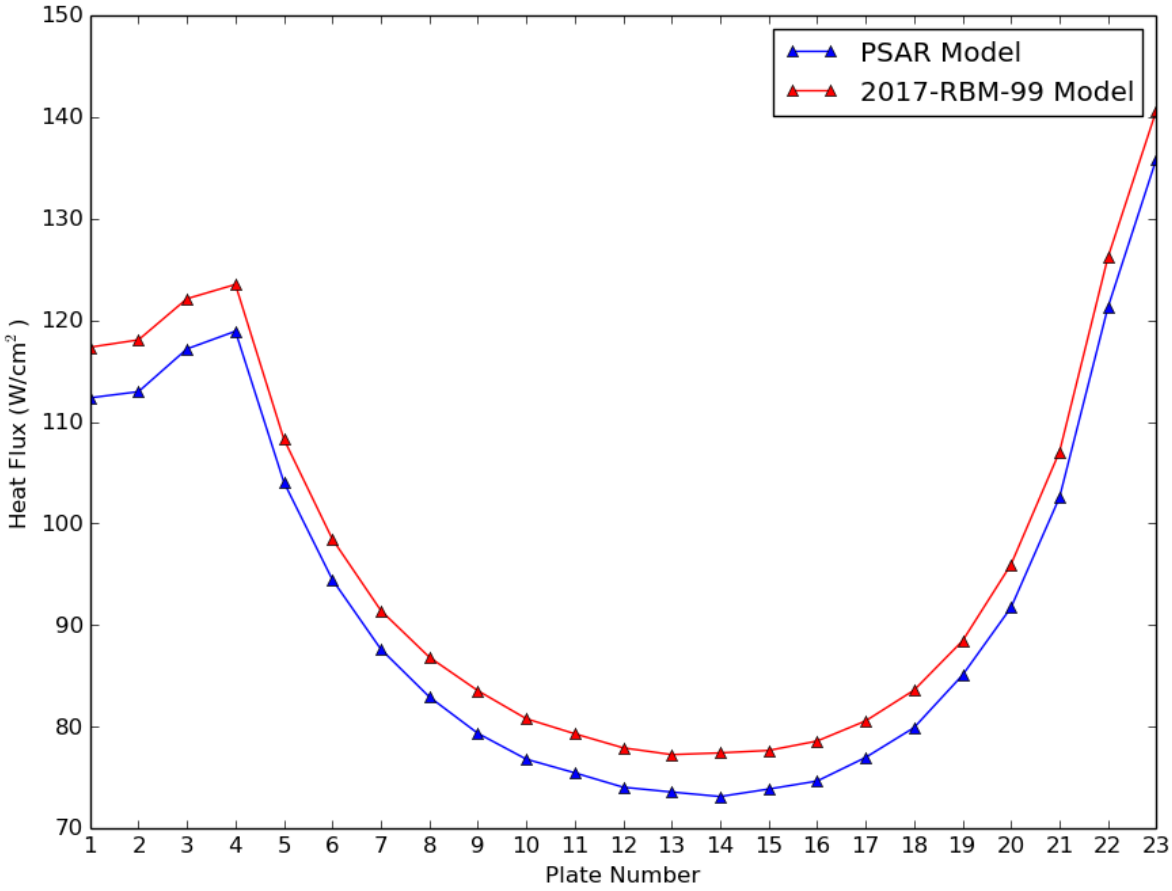

Figure 32: Axially-Averaged Heat Flux for PSAR and 2017-RBM-99 Models (Mixed-Burnup Eq. Xe Nominal Experiments)

Various core states were analyzed to find the reactor power for the onset of flow instability (OFI) condition with 2017-RBM-99 installed. Detailed power distributions for reference core states were evaluated using MCNP5. These reference core states varied the amount of power history for the elements in the reactor, the CFT sample loading, and the prior burnup history and potential skewing of the control blades. The power history was either all-fresh LEU (both BOC and equilibrium Xe) or the typical mixed-burnup core state (BOC, equilibrium Xe, and end-of-cycle (EOC). Fuel compositions for a mixed-burnup core that is typical for MURR operations were computed using REBUS-PC in the same manner as discussed in Chapter II. Two CFT configurations were analyzed: an empty experiment holder and a typical loaded experiment holder. Finally, a variation of two control blade parameters for a total of four

control blade conditions were considered. First, because the prior operating history of the control blades changes their reactivity worth and affects the axial power shape, both all-fresh blades and end-of-life blades were considered. Also, per MURR's technical specifications, two of the control blades are allowed have a 2.54 cm height delta compared to the two other blades, creating a "skew" condition. Consequently, the "nominal" case of four all-fresh banked blades was considered, along with three "skew" conditions, with two blades at their end-of-life burnup positioned higher than the two fresh blades. The end-of-life blades being at a higher axial position than the fresh blades creates greater shift in the power distribution.

In total, 40 LEU reference core states were modeled (80 if HEU is included). The work to execute them was split between ANL and MURR. The main challenge in executing these MCNP files was the need to find the critical blade heights for all of the reference cores. Because of the number of MCNP cases, finding the blade heights by hand was not feasible. A Python program was written to efficiently find the reference blade heights by executing models with lower numbers of particle histories, then bootstrapping those results until the full MCNP model was run. This program handled both the banked blade cases as well as the skewed blade cases.

The output files were processed at ANL to find the maximum heat flux. It was found that the axially-averaged heat flux was 238.5 W/cm^2 with 2017-RBM-99 installed versus 234.0 W/cm^2 that was calculated in the PSAR. These results were used for the OFI thermal analysis performed at ANL [18]. It was found that while 2017-RBM-99 does reduce the margin to safety, the safety criteria are easily met with 2017-RBM-99 installed.

C. CONCLUSIONS

In 2017, MURR, GA, and Nordion entered into a partnership agreement to produce fission-based ^{99}Mo. Because of the additional heat the 2017-RBM-99 device was expected to generate, as well as its impact on the core power distribution, safety analyses were completed to ensure that the margins to safety were still met with this device. While GA and Nordion withdrew from the partnership before 2017-RBM-99 was installed, this safety analysis was still completed to provide confidence to any other potential partners that a similar fission-based ^{99}Mo experiment would be feasible with both the HEU and LEU cores at MURR.

In the scope of this research there were two main objectives. First, this analysis provided confidence that the preliminary LEU fuel element design still provided adequate margins to safety with the instillation of 2017-RBM-99. In order to accurately gauge the impacts of the changes to the MURR core since the PSAR model was analyzed, this analysis also included determining the impacts of the current core configuration in comparison to the PSAR MCNP model. Heat flux and power shape calculations were done, and from these preliminary results it was determined that the preliminary LEU fuel element design was acceptable to move forward with until detailed safety analysis was done.

The second objective was finding the critical blade heights for approximately 40 LEU reference states so that power distributions could be analyzed for OFI analysis. While power distribution calculations are routine for this sort of analysis, finding the critical blade heights for this many MCNP input files with the limited computing power at MURR proved challenging. A Python program was written to efficiently iterate through multiple MCNP cases to determine the critical blade heights for each reference core state. Once the full model was run at the critical blade heights, power distributions were calculated from the MCNP tallies and provided to the thermal-hydraulics analysts. The thermal-hydraulics analysis done at ANL showed that while

margins to safety were reduced, the 2017-RBM-99 device still maintained an adequate margin to the previously established safety parameters [18].

This analysis also provided key insights into the transition core work discussed in Chapter II. While the transition core work did not assume the 2017-RBM-99 device was installed in the reactor, the method used to build the various core states using REBUS for the transition core work was similar to the method used to build the core states for the 2017-RBM-99 analysis. Also, the power distribution calculations that informed the OFI analysis was similar in both sets of analyses. While the transition core analysis and the 2017-RBM-99 analysis are focused on two different problems, the methods used to analyze these problems were similar in many ways.

V. CONCLUSIONS

In cooperation with the international non-proliferation community, the United States is committed to fighting terrorism by reducing the amount of weapons-grade nuclear material around the world. Towards that end, the US DOE NNSA supports a Reactor Conversion Program through the Office of Material Management and Minimization. As one of the six USHPRR in the United States, MURR is actively working to convert from the current HEU fuel to a high-density U-10Mo LEU fuel. As a part of this conversion, several areas of analyses have been completed, are underway, or are planned in the future. This dissertation describes the work done for three of these analyses: the startup test plan and prediction analysis, the transition cores analysis, and the potential fission-based molybdenum-99 production upgrade analysis.

As a part of the MURR's LEU licensing action, a startup test plan is required by the NRC. In support of the startup test plan, predictions were made for key reactor physics parameters for the all-fresh LEU core. These parameters include the approach to critical, primary coolant void coefficient of reactivity, flux trap void coefficient of reactivity, determination of flux trap sample reactivity worth, radial and axial thermal neutron flux mapping, primary and pool temperature coefficient of reactivity, and flux mapping of experimental positions. Predictions for these tests also included comparisons with measured HEU values and with MURR Technical Specification requirements, where applicable. This prediction analysis will support the startup tests by providing a baseline set of expectations and additional insight into the performance of the LEU core.

Once the all-fresh LEU core is characterized by the startup tests, MURR will begin full power operation with the new LEU fuel. Transition cores are those between the initial all-fresh

LEU core and the point at which MURR operates with a typical mixed-burnup fuel loading and has a nominal number of fuel elements in the active fuel inventory to support prototypic operations. During this period, MURR will operate atypically due to the lack of burned fuel elements and the reduced number of elements in the active fuel inventory. A Python program was developed to map a potential sequence to quickly move from this atypical operation to prototypic operations with LEU. This program incorporated MURR operational constraints, as well as factors such as element burnup limits, to create a realistic transition scheme.

Analysis was done to evaluate the impact of these transition cycles on experimental performance and impacts to established safety margins. It was found that by week 30, the BOC core burnup is within the nominal range of typical mixed-burnup core operation, and by week 75, there are 32 elements in the active fuel inventory. Even with a power uprate from 10 MW with HEU to 12 MW with LEU, experimental performance in some experiment positions is reduced relative to current performance with HEU, but meets or exceeds the HEU performance after week 23. It was further found that there is adequate margin to OFI during all transition cycles, which is a key thermal-hydraulics safety criterion.

As a medical isotope production facility, MURR is always seeking to improve and add capabilities to produce these isotopes. In support of this, GA and Nordion, with a partnership between GA and NNSA, entered into an agreement to develop the capability to produce fission-based ^{99}Mo at MURR. Because of the high fission power of this device (500 kW), further safety analysis was necessary to determine whether adequate margins to prior established safety criteria were still met with this device (named 2017-RBM-99) present in the reactor. Prior to this detailed analysis, preliminary scoping analysis was done to give confidence as to whether the

preliminary LEU fuel element design was a viable design to move forward with to LEU conversion.

The preliminary analysis determined that the preliminary LEU fuel element design was viable moving forward. This analysis found that the experiment holder change in the CFT provided more margin to safety by shifting the power towards the inner fuel plates and away from the outside plates. From that point, detailed safety analysis was done to support the insertion of the 2017-RBM-99 device. 40 reference core states were studied for the LEU core, with various core burnups, flux trap configurations, and control blade burnups and skews. After determining the critical control blade positions for the core states, the hot-stripe heat flux results were used in the thermal-hydraulics analysis, which was completed at ANL. The thermal-hydraulic analysis showed that while margins to safety were reduced from the insertion of 2017-RBM-99, adequate safety margins were still met with the ^{99}Mo device.

As MURR moves towards LEU conversion, these analyses will play a critical role in the realization of that goal. While good progress has been made, there is still more to do in the future with these analyses. The startup test plan and prediction analysis presented in Chapter II will be codified into a procedure for MURR operations to follow at the time of conversion, and both the procedure and the test plan and predictions will become a MURR technical document that is now being drafted. The transition core analysis will need to be confirmed with the MURR core layout, experiment loading, and control blade power history as LEU conversion approaches. Finally, should fission-based ^{99}Mo production be pursued to MURR, analysis will need to be done to confirm that the analysis done in Chapter IV, and the broader analysis done at ANL, is sufficient for the particular device that will be inserted into MURR. While future work will need

to be done, this research makes significant progress in the realization of converting MURR to LEU fuel.

VI. REFERENCES

[1] E. H. Wilson, *et al*, "U. S. High Performance Research Reactor Conversion Program: An Overview on Element Design," in *Proceedings from the European Research Reactor Conference (RRFM)*, Rotterdam, Netherlands, 2017.

[2] J. A. Morman, F. Puig and J. G. Stevens, "Conversion of the Nigerian MNSR to Low Enriched Uranium Fuel," in *Proceedings from the Institute of Nuclear Materials Management Annual Meeting*, Palm Desert, California, 2019.

[3] E. H. Wilson, "U. S. High Performance Research Reactor Preliminary Design Milestone for Conversion to Low Enriched uranium Fuel," in *Proceedings from the European Research Reactor Conference (RRFM)*, Vol. 3, pp. 10, Sweimah, Jordan, 2019.

[4] B. Rabin, *et al*, "Preliminary Report on U-Mo Monolithic Fuel for Research Reactors," INL EXT-17-40975, Rev. 3, Idaho National Laboratory, Idaho Falls, Idaho, 2020.

[5] D. Chandler, "Neutronic and Thermal-Hydraulic Feasibility Studies for High Flux Isotope Reactor Conversion to Low-Enriched Uranium Silicide Dispersion Fuel," *Annals of Nuclear Energy,* no. 130, p. 277, 2019.

[6] E. E. Feldman, *et al*, "Technical Basis in Support of the Conversion of the University of Missouri Research Reactor (MURR) Core from Highly-Enriched Uranium to Low Enriched Uranium - Steady-State Thermal-Hydraulic Analysis," ANL/RERTR/TM-12-37 Rev. 1, Argonne National Laboratory, Lemont, Illinois, 2013.

[7] J. A. Stillman, *et al*, "Low Enriched Uranium Conversion Preliminary Safety Analysis Report for the University of Missouri Research Reactor," University of Missouri Research Reactor, Columbia, Missouri, 2017.

[8] J. A. Stillman, *et al*, "Technical Basis in Support of the Conversion of the University of Missouri Research Reacotr (MURR) Core from Highly-Enriched Uranium to Low Enriched Uranium - Core Neutron Physics," ANL/RERTR/TM-12-30, Argonne National Laboratory, Lemont, Illinois, 2012.

[9] D. D. Senor and D. Burkes, "Fuel Fabrication Capability Research and Development Plan," PNNL-22528 Rev. 1, Pacific Northwest National Laboratory, Richland, Washington, 2014.

[10] R. E. Johnson and e. al, "UMo Foil Fabrication Demonstration Line at Babcock & Wilcox," in *Proceedings from the European Research Reactor Conference (RRFM)*, Bucharest, Romania, 2015.

[11] E. H. Wilson, *et al*, "Preliminary Fuel Development and Reactor Design Milestones for LEU Conversion of U. S. High Performance Research Reactors," in *Proceedings from International Conference on Nuclear Security*, Vienna, Austria, 2020.

[12] X-5 Monte Carlo Team, "MCNP - Version 5, Vol. I: Overview and Theory," LA-UR-03-1987, Los Alamos National Laboratory, Los Alamos, New Mexico, 2003.

[13] F. B. Brown, *et al*, "Verification of MCNP5-1.60," LA-UR-10-05611, Los Alamos National Laboratory, Los Alamos, New Mexico, 2010.

[14] A. P. Olson, "A User's Guide for the REBUS-PC Code, Version 1.4," ANL/RTR/TM-19/13, Argonne National Laboratory, Lemont, Illinois, 2001.

[15] J. R. Deen, *et al*, "WIMS-ANL User Manual, Rev. 3," ANL/RERTR/TM-23 Rev. 3, Argonne National Laboratory, Lemont, Illinois, 1999.

[16] B. Dionne, J. A. Stillman and J. Stevens, "Applicability of WIMS-ANL to Generate Cross Sections for Very High Density UMo Fuel in Proposed LEU Fuel Assembly," in *Proceedings from the 2008 International Meeting on Reduced Enrichment for Research and Test Reactors*, Washington, D. C., 2008.

[17] N. J. Peters and K. Kutikkad, "Novel Methodologies for Modeling the Net Fission-Poison Reactivity Transients to Accurately Predict Criticals and Hot-Startup ECPs for the MURR Core," *Nuclear Technology,* vol. 201, no. 1, pp. 80-98, 2018.

[18] J. A. Stillman , *et al*, "Safety Analysis of the Mo-99 Production Upgrade of the University of Missouri Research Reactor (MURR) with Highly Enriched and Low-Enriched Uranium Fuel," ANL/RERTR/TM-18-16, Argonne National Laboratory, Lemont, Illinois, 2019.

[19] Office of Nuclear Reactor Regulation, "Guidelines for Preparing and Reviewing Applications for the Licensing of Non-Power Reactors," NUREG-1537, Part 1, Nuclear Regulatory Commission, Washington, D.C., 1996.

[20] C. Julian, "Evaluation of a 6.2 Kilogram U235 Core Loading for the Missouri University Research Reactor," University of Missouri Research Reactor, Columbia, Missouri, 1970.

[21] C. Julian, "Low Power Testing Program for the Missouri University Research Reactor 6.2 Kilogram Core," University of Missouri Research Reactor, Columbia, Missouri, 1971.

[22] E. Wilson, *et al*, "Comparison and Validation of HEU and LEU Modeling Results to HEU Experimental Benchmark Data for the Massachusetts Institute of Technology MITR Reactor," ANL/RERTR/TM-10-41, Argonne National Laboratory, Lemont, Illinois, 2010.

[23] D. J. Diamond and A. Varuttamaseni, "A Reload and Startup Plan for Conversion of the NIST Reactor," BNL-112005-2016-IR-R1, Brookhaven National Laboratory, Upton, New York, 2017.

[24] J. R. White and e. al, "Calculational Support for the Startup of the LUE-Fueled UMass-Lowell Research Reactor," in *Proceedings from PHYSOR 2000*, Pittsburg, Pennsylvania, 2000.

[25] University of Missouri Research Reactor, "Technical Specifications for the University of Missouri Research Reactor," Facility Operating Licencse No. R-103, Appendix A, University of Missouri Research Reactor, Columbia, Missouri.

[26] The Aluminum Association, "International Alloy Designations and Chemical Composition Limits for Wrought Aluminum and Wrought Aluminum Alloys," The Aluminum Association, Alexandria, Virginia, 2015.

[27] National Research Council (US) Committee on Medical Isotope Production Without Highly Enriched Uranium, "Medical Isotope Production Without Highly Enrched Uranium," National Academies Press, Washington, D.C., 2009.

[28] Boston Scientific, "Product Specifications: TheraSphere," [Online]. Available: https://www.bostonscientific.com/en-US/products/cancer-therapies/therasphere-y90-glass-microspheres/product-specifications.html.

[29] MIT Nuclear Reactor Laboratory, "Safety Analysis Report for the MIT Research Reactor (MITR-III) Rev. 1," Massachusetts Institute of Technology, Cambridge, Massachusetts, 2000.

[30] ASTM International, "Standard Practice for Determining Neutron Fluence, Fluence Rate, and Spectra by Radioactivation Techniques," ASTM E261-16, ASTM International, West Conshohocken, Pennsylvania, 2016.

[31] L. Foyto, *et al*, "CD35 Low-Enriched Uranium Transition Fuel Cycle Report," TDR-0138, University of Missouri Research Reactor, Columbia, Missouri, 2013.

[32] W. Cowherd, *et al*, "Transition Core Analysis for HEU to LEU Fuel Conversion at the University of Missouri Research Reactor," *Nuclear Technology,* (to be published).

[33] Lantheus Medical Imaging, "Quadramet," [Online]. Available: https://www.lantheus.com/products/overview/quadramet/. [Accessed 2 June 2020].

[34] Advanced Accelerator Applications, "Lutathera," Advanced Accelerator Applications, [Online]. Available: https://lutathera.com/. [Accessed 2 June 2020].

Appendix A

As discussed in Chapter III, a Python program was written to select the core loading for the transition cores. Attached is the executable code (CoreLoading.py) and the class that holds the core inventory information (CoreInventory.py), along with inline comments to explain the program.

CoreLoading.py

```
'''
This is the executable file for running the LEU Core Loading for MURR.
Created by: Wilson Cowherd
'''
import os
import csv
import math
import matplotlib.pyplot as plt
import numpy
import itertools
import string
from collections import OrderedDict
from CoreInventory import CoreInventory

# Initialize the elements for the first 6 weeks
elementList = []
element_pos = {}
for i in range(1):
    for j in range(1, 9):
        elementList.append(string.ascii_uppercase[i] + str(j))
# Add the burnup for the first 6 weeks
cycles = OrderedDict()
coreburnup = [37.8 * x for x in range(6)]
# Create the Core Inventory and add elements to it
coreInventory = CoreInventory()
coreInventory.addElements(elementList[:8], [1] * 8)
week = 1
letter = 1
number = 1
# Add the cycle number for the first 6 weeks
```

```
31 for i in range(week, 7):
32     if i <= 6:
33         if i > 1:
34             coreInventory.addCycles(elementList[:8], [i] * 8)
35         cycles[week] = elementList[:8]
36     for key in cycles.keys():
37         coreInventory.addBurnup(cycles[key], [9.45] * 8)
38
39 element_pos['A1'] = ['X1'] * 6
40 element_pos['A2'] = ['X5'] * 6
41 element_pos['A3'] = ['X2'] * 6
42 element_pos['A4'] = ['X6'] * 6
43 element_pos['A5'] = ['X3'] * 6
44 element_pos['A6'] = ['X7'] * 6
45 element_pos['A7'] = ['X4'] * 6
46 element_pos['A8'] = ['X8'] * 6
47
48 # Method for creating a new element
49 def createNewElements(i, j):
50     if i < len(string.ascii_uppercase):
51         newElement1 = string.ascii_uppercase[i] + str(j)
52         newElement2 = string.ascii_uppercase[i] + str(j + 1)
53     else:
54         newElement1 = string.ascii_uppercase[int(i / len(string.ascii_uppercase))] +
       string.ascii_uppercase[
55             i % len(string.ascii_uppercase)] + str(j)
56         newElement2 = string.ascii_uppercase[int(i / len(string.ascii_uppercase))] +
       string.ascii_uppercase[
57             i % len(string.ascii_uppercase)] + str(j + 1)
58     return [newElement1, newElement2]
59
60 # Method for checking the burnup to make sure that elements are not at the max MWd
61 def checkBurnup():
62     burnup = coreInventory.getBurnup()
63     tmp = []
64     for element in burnup.keys():
65         if burnup[element] < 179:
66             tmp.extend([element, coreInventory.getElements()[element]])
67     return tmp
68
69 # Method for building the best core possible
70 def buildCore(elements_available, curr_cycle):
71     leading_elements = elements_available[::2]
72     # This variable holds all the possible combos of 4 pairs of elements for a core loading
73     possiblecombos = list(itertools.combinations(leading_elements, 4))
74     working_combos = []
```

```
75  best_core = []
76  prev_cycles = {}
77  # This for loops determines how many possible combos there are by determining if they
    were in the last cycle
78  for combo in possiblecombos:
79      matches = 0
80      for j in range(len(combo)):
81          if coreInventory.getCycles()[combo[j]][-1] == curr_cycle - 1:
82              matches += 1
83      prev_cycles[combo] = matches
84  best_burnup = 0
85  includeFreshElements = False
86  # If there are no working combos, tell program to include fresh elements
87  for combo in possiblecombos:
88      for j in range(len(combo)):
89          if coreInventory.getBurnup()[combo[j]] == 0:
90              includeFreshElements = True
91              break
92  # Further trim working possible combos by determining their core burnup and how many
    elements were in the
93  # previous cycle
94  for combo in possiblecombos:
95      if includeFreshElements:
96          if coreInventory.getBurnup()[combo[0]] != 0 and
    coreInventory.getBurnup()[combo[1]] != 0 and \
97                  coreInventory.getBurnup()[combo[2]] != 0 and
    coreInventory.getBurnup()[combo[3]] != 0:
98              pass
99          elif sum([coreInventory.getBurnup()[combo[0]],
    coreInventory.getBurnup()[combo[1]],
100                 coreInventory.getBurnup()[combo[2]],
101                 coreInventory.getBurnup()[combo[3]]]) > 226 and prev_cycles[combo] >= 2:
102             pass
103         else:
104             working_combos.append(combo)
105     else:
106         if prev_cycles[combo] == 4:
107             pass
108         elif sum([coreInventory.getBurnup()[combo[0]],
    coreInventory.getBurnup()[combo[1]],
109                 coreInventory.getBurnup()[combo[2]],
110                 coreInventory.getBurnup()[combo[3]]]) > 226 and prev_cycles[combo] >= 2:
111             pass
112         else:
113             working_combos.append(combo)
```

```
114     # This loop runs until it finds the best working core, if possible. If not, it will return to the
        main method
115     # and add a fresh pair of elements. If the user wants to allow elements to be in the core
        from a previous cycle
116     # change the "elif max_previous_cycle <" condition.
117     running = True
118     max_previous_cycles = 0
119     while running:
120         for combo in working_combos:
121             if len(best_core) == 0 and sum([coreInventory.getBurnup()[combo[0]],
        coreInventory.getBurnup()[combo[1]],
122                                             coreInventory.getBurnup()[combo[2]],
123                                             coreInventory.getBurnup()[combo[3]]]) < 356 and prev_cycles[
124                 combo] <= max_previous_cycles:
125                 best_core = combo
126                 best_burnup = sum([coreInventory.getBurnup()[combo[0]],
        coreInventory.getBurnup()[combo[1]],
127                                    coreInventory.getBurnup()[combo[2]],
        coreInventory.getBurnup()[combo[3]]])
128             elif len(best_core) > 0 and sum([coreInventory.getBurnup()[combo[0]],
        coreInventory.getBurnup()[combo[1]],
129                                              coreInventory.getBurnup()[combo[2]],
130                                              coreInventory.getBurnup()[combo[3]]]) < 356 and prev_cycles[
131                 combo] <= max_previous_cycles:
132                 burnup = sum([coreInventory.getBurnup()[combo[0]],
        coreInventory.getBurnup()[combo[1]],
133                               coreInventory.getBurnup()[combo[2]],
        coreInventory.getBurnup()[combo[3]]])
134                 if math.fabs(burnup - 343) < math.fabs(best_burnup - 343):
135                     best_burnup = burnup
136                     best_core = combo
137         if 330 <= best_burnup <= 356:
138             running = False
139         elif max_previous_cycles < 0:
140             max_previous_cycles += 1
141         else:
142             running = False
143     # Returns to the main method the best core found. If the list is empty, the main method
        will run again after
144     # adding a fresh pair of elements
145     core = []
146     for i in best_core:
147         core.extend([i, coreInventory.getElements()[i]])
148     coreburnup.append(best_burnup)
149     return core
150
```

```
# This determines the position of elements in the core based on their burnup.
def setCorePos(curr_core):
    core_pos = ['X2', 'X6', 'X4', 'X8', 'X3', 'X7', 'X1', 'X5']
    all_elements = coreInventory.getBurnup()
    a = 0
    for element in all_elements:
        if element not in curr_core:
            if element_pos[element] != []:
                tmp1 = element_pos[element]
                tmp1.append('')
                tmp2 = element_pos[coreInventory.getElements()[element]]
                tmp2.append('')
                element_pos[element] = tmp1
                element_pos[coreInventory.getElements()[element]] = tmp2
        else:
            tmp1 = element_pos[element]
            tmp1.append(core_pos[a])
            tmp2 = element_pos[coreInventory.getElements()[element]]
            tmp2.append(core_pos[a + 1])
            element_pos[element] = tmp1
            element_pos[coreInventory.getElements()[element]] = tmp2
            a += 2

# Starting and ending week determine how long the program will run after the first 6 weeks
startingweek = 7
endingweek = 52 * 3

num_of_elements = [8] * 6       # This list keeps track of how many elements are in the core inventory
for i in range(startingweek, endingweek + 1):
    availableElements = checkBurnup() # Check burnup to remove elements over the MWd limit
    # This "if" statement slowly builds the core inventory to 32 elements. If all the conditions in the
    # statement are met, the program will add a new element
    if (len(availableElements) < 32 and i % 5 == 0 and i <= 52) or (len(availableElements) < 32 and i % 3 == 0 and 52 < i <= 75) or (len(availableElements) < 32 and i > 75):
        newelements = createNewElements(letter, number)
        coreInventory.addElements(newelements, [[], []])
        availableElements.extend(newelements)
        elementList.extend(newelements)
        element_pos[newelements[0]] = []
        element_pos[newelements[1]] = []
        number += 2
        if number > 8:
            number = 1
```

```
193             letter += 1
194     keepRunning = True
195     # This builds the core for the individual weeks
196     while keepRunning:
197         core = buildCore(availableElements, i) # Calls the build core method
198         core = sorted(core)
199         # If the length of the returned core is 0, add fresh elements
200         if len(core) == 0:
201             newelements = createNewElements(letter, number)
202             coreInventory.addElements(newelements, [[], []])
203             availableElements.extend(newelements)
204             elementList.extend(newelements)
205             element_pos[newelements[0]] = []
206             element_pos[newelements[1]] = []
207             number += 2
208             if number > 8:
209                 number = 1
210                 letter += 1
211     # If a suitable core is found, add the elements to the core inventory and keep track of the
        cycle they were in
212         else:
213             setCorePos(core)
214             print 'Week ' + str(i) + ': ', len(availableElements)
215             num_of_elements.append(len(availableElements))
216             cycles[i] = core
217             coreInventory.addBurnup(cycles[i], [9.45] * 8)
218             coreInventory.addCycles(cycles[i], [i] * 8)
219             keepRunning = False
220
221 # Method graphs the core burnup over the number of weeks
222 def graphCoreBurnup(burnuplist):
223     burnuplist.insert(0, 0)
224     burnuplist.insert(6,0)
225     plt.xlabel('Weeks')
226     plt.ylabel('Total Core Burnup')
227     plt.title('Core Burnup (Target 32 Elements)')
228     plt.plot(numpy.linspace(1, len(burnuplist), len(burnuplist)), burnuplist)
229     plt.show()
230
231 # These two "for" loops create two lists: The element IDs and the core bunrup
232 coreburnup = [x * 2 for x in coreburnup if x != 0]
233 first_row = ['Element ID']
234 for i in range(1, (52 * 4) + 1):
235     first_row.append('Cycle ' + str(i))
236 for element in coreInventory.getCycles().keys():
237     if coreInventory.getCycles()[element][1] > 4:
```

```
238         tmp1 = element_pos[element]
239         tmp3 = element_pos[coreInventory.getElements()[element]]
240         for i in range(coreInventory.getCycles()[element][1] - 1):
241             tmp1.insert(0, '')
242             tmp3.insert(0, '')
243         element_pos[element] = tmp1
244         element_pos[coreInventory.getElements()[element]] = tmp3
245
246 # This method creates a csv file that can be easily imported into Excel to view the element
        use over time
247 with open('core_loading5.csv', 'w') as csvfile:
248     file_writer = csv.writer(csvfile)
249     file_writer.writerow(first_row)
250     for key in element_pos.keys():
251         element1 = [key]
252         for items in element_pos[key]:
253             element1.append(items)
254         file_writer.writerow(element1)
255     file_writer.writerow(coreburnup)
256     file_writer.writerow(num_of_elements)
257
258 graphCoreBurnup(coreburnup)
```

CoreInventory.py

```
 1 '''
 2 This class is the base for the CoreLoading.py main executing script. This class houses all the
       info about element
 3 burnup, cycles, and IDs
 4 '''
 5
 6 from collections import OrderedDict
 7
 8 class CoreInventory:
 9
10     def __init__(self):
11
12         self.elements = OrderedDict()
13         self.burnup = OrderedDict()
14         self.cycles = {}
15
16     # Add Elements to core inventory
17     def addElements(self,elementList,cycleList):
```

```
18      for i in range(0,len(elementList),2):
19          self.elements[elementList[i]] = elementList[i+1]
20          self.burnup[elementList[i]] = 0
21          self.cycles[elementList[i]] = [cycleList[i]]
22      self.sortElements()
23
24  # Return the List of Elements
25  def getElements(self):
26      return self.elements
27
28  # Add burnup to the elements in a particule cycle
29  def addBurnup(self,elementList,burnupList):
30      for i in range(0,len(elementList),2):
31          tmp = self.burnup[elementList[i]] + burnupList[i]
32          self.burnup[elementList[i]] = tmp
33      self.sortElements()
34
35  # Get the burnup of the elements
36  def getBurnup(self):
37      return self.burnup
38
39  # Add the cycle number to an element
40  def addCycles(self,elementList,cycleList):
41      for i in range(0,len(elementList),2):
42          tmp = self.cycles[elementList[i]]
43          tmp.append(cycleList[i])
44          self.cycles[elementList[i]] = tmp
45
46  # Return the cycles the elements were in
47  def getCycles(self):
48      return self.cycles
49
50  # Sort elements based on bunrup
51  def sortElements(self):
52      self.burnup = OrderedDict(reversed(sorted(self.burnup.items(), key=lambda t: t[1])))
53      tmp = OrderedDict()
54      for key in self.burnup.keys():
55          tmp[key] = self.elements[key]
56
57      self.elements = tmp
58
59  # Remove an element from the core inventory
60  def removeElement(self,elementList):
61      for i in range(0,len(elementList),2):
62          del self.elements[i]
```

VITA

Wilson Cowherd was born in Mount Vernon, Missouri on February 22, 1991. He grew up in Mount Vernon, graduating from Mount Vernon High School in 2009 in the top ten in his class. He went on to study physics and mathematics at Drury University in Springfield, Missouri. He was awarded a Bright Flight Scholarship and Presidential Scholarship and played baseball for Drury University. He graduated cum laude in 2013 while being named the most outstanding senior in both the physics and mathematics departments.

Wilson went on to study Nuclear Engineering at the University of Missouri, with a research focus on the maximum hypothetical accident analysis for the highly-enriched uranium (HEU) to low enriched uranium (LEU) fuel conversion at the University of Missouri Research Reactor (MURR). Wilson graduated with a MS in Nuclear Engineering from the University of Missouri in 2014.

Wilson then went on to work as a Neutronics Analyst at the Idaho National Laboratory (INL) from January 2015 to July 2017. While there he focused on experiment analysis for the Advanced Test Reactor (ATR). He supported a variety of experiment types from many programs. He authored or coauthored a number of experiment reports, conference papers, and presented at a number of national conferences for his work on experiments at INL.

From August 2017 to July 2020, Wilson did his PhD research in Nuclear Engineering at the University of Missouri, again working with MURR in support of their HEU to LEU fuel conversion. For this research, he focused on the startup, transition cores, and molybdenum-99 experiment upgrade analyses for the HEU to LEU fuel conversion. Currently, Wilson resides in Hinsdale, Illinois and works for Argonne National Laboratory as a Nuclear Engineer, supporting reactor fuel conversion efforts.